



CATOLICA
ESCOLA SUPERIOR DE BIOTECNOLOGIA

PORTO

ANALYSIS OF SOUND-INDUCED
ANGIOGENESIS IN THE DEVELOPMENT
OF A 3D TUMOR MODEL

by

Margarida Alice Leal Coelho Barbosa

November 2024



CATÓLICA
ESCOLA SUPERIOR DE BIOTECNOLOGIA

PORTO

ANALYSIS OF SOUND-INDUCED ANGIOGENESIS IN THE DEVELOPMENT OF A 3D TUMOR MODEL

Training Placement Report presented to *Escola Superior de Biotecnologia* of the
Universidade Católica Portuguesa to fulfill the requirements of Master of Science degree in
Biomedical Engineering

by

Margarida Alice Leal Coelho Barbosa

Supervisor (Company): Prof. Dr. Michael Raghunath

Tutor (University): Prof. Dr. Viviana Ribeiro

November 2024

“What has a price can be replaced by something else as its equivalent; what on the other hand is raised above all price and therefore admits of no equivalent has a dignity.”

— Immanuel Kant

Resumo

O ambiente tumoral gera o aparecimento de células com o mecanismo alterado e crescimento descontrolado. O recurso a mecanismos que resultam na sua expansão é o que lhes permite um crescimento indefinido e evolução. A angiogénese tumoral é um dos mecanismos utilizados por células cancerígenas de forma a sobreviverem, expandirem-se e estabelecerem o seu próprio ambiente.

Através das células tumorais, são secretados diversos fatores em resposta à hipoxia e à necessidade de nutrientes, resultante do crescimento rápido e multiplicação por parte típica destas células. A angiogénese, com a formação de novos vasos sanguíneos, surge não só para colmatar estas necessidades, mas também para criar um microambiente que facilite a invasão e disseminação das células cancerígenas para outros tecidos, desempenhando um papel crucial no crescimento e metastização de tumores.

Com a criação de um modelo 3D onde está presente o ambiente tumoral, este trabalho tem como perspectiva observar este mecanismo. Para isso, recorre à utilização da bioacústica, através de ondas sonoras e vibrações a uma determinada frequência e aceleração, determina o rearranjo celular.

Assim, através de um modelo 3D constituído por duas camadas distintas, sendo uma formada por células endoteliais em combinação com células mesenquimais, e uma camada superior, constituída por células de cancro da mama, este trabalho tem como objetivo analisar a influência da presença de células cancerígenas, nomeadamente ao nível da promoção de sprouting por parte das células endoteliais, e assim o início do mecanismo angiogénico.

Modelo Tumoral 3D, Angiogénese, Indução Sonora

Abstract

The tumor environment arises the appearance of cells with altered mechanisms and uncontrolled growth. The use of mechanisms that result in their expansion is what allows them to grow indefinitely and evolve. Tumor angiogenesis is one of the mechanisms used by cancer cells to survive, expand and establish their own environment.

Through tumor cells, several factors are secreted in response to hypoxia and the need for nutrients, resulting from the rapid growth and multiplication typical of these cells. Angiogenesis, with the formation of new blood vessels, arises not only to meet these needs, but also to create a microenvironment that facilitates the invasion and spread of cancer cells to other tissues, playing a crucial role in the growth and metastasis of tumors.

By creating a 3D model where the tumor environment is present, this work aims to observe this mechanism. To do so, it uses bioacoustics, through sound waves and vibrations at a certain frequency and acceleration, to determine cellular rearrangement.

Thus, through a 3D model consisting of two distinct layers, one formed by endothelial cells in combination with mesenchymal cells, and a top layer, consisting of breast cancer cells, this work aims to analyze the influence of the presence of cancer cells, namely at the level of the promotion of sprouting by endothelial cells, and thus the initiation of the angiogenic mechanism.

3D Tumor Model, Angiogenesis, Sound Induced

Acknowledges

I would like to express my heartfelt gratitude to Prof. Dr. Michael Raghunath for warmly welcoming me into his lab and offering support whenever I needed it, always with kindness and encouragement, which allowed me to have one of the most significant experiences of my life. I am also deeply thankful to Bianca Fischli and Britta Striegl, whose invaluable assistance and constant support throughout these months were essential to the completion of this work.

I am sincerely grateful to Prof. Dr. Viviana Ribeiro for her invaluable guidance and support, which helped me gain clarity in my thinking and approach challenges with patience and resilience. Her willingness to assist me with anything I needed, even beyond thesis-related matters, is something for which I will always be deeply grateful.

I want to express my deepest gratitude to those who have given me everything I needed to reach this point. My heartfelt thanks go to my mother, Quitéria, and my grandmother, Maria Alice, for being examples of strength and independence, and to my uncle, Abílio, for his kindness and generosity. I will always admire you.

To Tiago, thank you for your love, friendship, and unwavering support whenever I needed it. These past years would not have been as meaningful without you. To my sister, Maria João, thank you for being my best friend and one of the people I admire most. To Inês, who is like a sister to me, and to Filipe, who has felt like a brother from the beginning and has always been there to help—thank you. Though they don't even know how to talk yet, Frederica and Francisco already hold a special place in my heart and have brightened my life. I am also deeply grateful to my aunt and godmother, Teresa, and my uncle, Florêncio, who have been a constant source of love and support, as well as to my godfather, Pedro, who feels like an older brother.

Lastly, to my friends Beatriz, Joana, Miguel, Carina, Henrique, and Matilde—thank you for standing by me every step of the way.

Love you all.

Table of Contents

RESUMO	VII
ABSTRACT	IX
ACKNOWLEDGES	XI
LIST OF FIGURES	XVI
LIST OF TABLES	XIX
LIST OF ABBREVIATIONS	XXI
1.1. BREAST CANCER	2
1.2 TUMOR MICROENVIRONMENT	3
1.2.1. EXTRACELLULAR MATRIX	3
1.2.2. CELLULAR COMPONENTS.....	5
1.3. ANGIOGENESIS	9
1.3.1. MECHANISMS INVOLVED IN ANGIOGENESIS	10
1.3.2 ANGIOGENIC FACTORS	12
1.4. ROLE OF ENDOTHELIAL CELLS	13
1.5. ROLE OF MSC	14
1.6. THEORETICAL BACKGROUND	15
1.6.1. 2D vs 3D MODELS.....	15
1.6.2. CELLULAR SPHEROIDS MODELS	16
1.6.3. ACOUSTIC MANIPULATION.....	16
1.6.4. TUMOR ANGIOGENESIS MODELS IN VITRO.....	18
1.7. HYPOTHESIS	20
CHAPTER 2: MATERIALS AND METHODS	21
2.1. CULTIVATION OF SAOS-2	21
2.2. CULTIVATION OF MDA-MB-231	21
2.3. CULTIVATION OF HUVECS	21
2.4. CULTIVATION OF MSC	21
2.5. CULTURE OF SPHEROIDS	22
2.6. PREPARATION OF THE GELATIN HYDROGEL	22
2.7. PREPARATIONS OF THE INSERTS	22
2.8. IMAGING	24
CHAPTER 3: RESULTS	25
3.1. SPHEROIDS FORMATION	25
3.1.1. SAOS-2	25

3.1.2. MDA-MB-231.....	26
3.1.3. GFP-HUVEC: MSC (5:1).....	26
3.1.4. GFP-HUVEC:MSC (1:3).....	27
3.2. SYSTEM OPTIMIZATION WITH SAOS-2	28
3.3. OBSERVATION OF SPROUTING FORMATION	29
3.3.1. 5:1 Co-CULTIVATION OF GFP-HUVEC AND MSC	29
3.3.2. 5:1 Co-CULTIVATION OF GFP-HUVECS AND MSC WITHOUT SIM	33
3.3.3. 1:3 Co-CULTIVATION OF GFP-HUVECS AND MSC	35
 <u>CHAPTER 4: DISCUSSION</u>	 <u>37</u>
 <u>CHAPTER 5: CONCLUSIONS AND FUTURE PROSPECTS.....</u>	 <u>41</u>
 <u>BIBLIOGRAPHY.....</u>	 <u>42</u>

List Of Figures

Chapter 1

- Figure 1.1 Overview of the classifications of Breast Cancer
- Figure 1.2 Remodeling of the ECM on a primary tumor
- Figure 1.3 The microenvironment that surrounds cancer cells in a primary tumor
- Figure 1.4 The Role of TAMS in the tumor microenvironment
- Figure 1.5 CAFs in the tumor Microenvironment
- Figure 1.6 Different modes of Angiogenesis
- Figure 1.7 Inducers and inhibitors of Angiogenesis that affect the regular mechanism
- Figure 1.8 Interaction between MSC and cancer cells
- Figure 1.9 Schematic representation of the SIM process

Chapter 2:

- Figure 2.1 Pictures of the Cymatix, the SIM used. Show the overview of the machine. Display where the parameters of the pattern could be changed. Display showing the patterning being formed. A picture of the petri inside the machine taking by the Cymatix

Chapter 3:

- Figure 3.1. SAOS-2 Spheroids
- Figure 3.2 Spheroids formed with MDA-MB-231 at different concentrations
- Figure 3.3 GFP-HUVEC and MSC Spheroids (5:1)
- Figure 3.4 GFP-HUVEC and MSC Spheroids (1:3)
- Figure 3.5. These pictures were taken with the integrated camera in the CymatiX without backlight after the machine being turned on
- Figure 3.6. Due to the difficulty of obtaining a complete overview of the petri dish, screenshots were taken of the outer concentric ring
- Figure 3.7 Comparison between day 1 and day 8 on the sprout formation in all the concentric rings
- Figure 3.8 Evaluation of the sprout formation towards the days until day 8 on 5:1, HUVEC:MSC
- Figure 3.9 Evaluation of the sprout formation towards the days until day 3 on 5:1, HUVEC:MSC

Figure 3.10 Different levels of focus on the sprouts on the samples exposed to the SIM

Figure 3.11 Evaluation of the sprout formation towards the days until day 8 on 5:1, HUVEC:MSC that was not exposed to the SIM

Figure 3.12 Different levels of focus on the sprouts on the sample not exposed to the SIM

Figure 3.13. Due to the difficulty of obtaining a complete overview of the petri dish, screenshots were taken of all three concentric rings in the respective order from the inner circle to the outer one. A picture of a single spheroid was also taken

List Of Tables

Chapter 1:

Table 1 Growth factors involved in angiogenesis

Chapter 2:

Table 2.1 Descripton of the constitution of the SAOS-2 insert

Table 2.2. Descripton of the constitution of the HUVEC:MSC and BCC insert

List Of Abbreviations

2-dimensional (2D)

3-dimensional (3D)

Breast cancer cells (BCC)

Cancer-associated fibroblasts (CAFs)

Cytotoxic T-cells (CD8+)

Dendritic Cells (DC)

Epidermal Growth Factor (EGF)

Epidermal growth factor receptor 2 (HER2)

Epithelial–mesenchymal transition (EMT)

Extracellular matrix (ECM)

Fetal bovine serum (FBS)

Fibroblast growth factor (FGFs)

Foreskin tissue endothelial cells (HDMECs)

Green fluorescent protein-expressing Human Umbilical Vein Endothelial Cells (GFP-HUVEC)

Human umbilical veins endothelial cells (HUVECs)

Hypoxia-inducible factors (HIFs)

Hypoxia inducible factor 1 alpha (HIF-1 α)

Hepatocyte growth factor (HGF)

Insulin-like growth factor 1 (IGF1)

Interferon gamma (IFN- γ)

Interleukin-2 (IL-2)

Interleukin-10 (IL-10)

Matrix metalloproteases (MMPs)

Myeloid-derived suppressor cells (MDSC)

Mesenchymal stem cells (MSC)

Microbial transglutaminase (MTGase)

Natural killer (NK)

Placenta growth factor (PlGF)

Platelet-Derived Growth Factor (PDGF)

Phosphate buffered saline (PBS)

Regulatory T cells (Tregs)

Sarcoma Osteogenic-2 (SAOS-2)
Sound Induced Morphology (SIM)
T helper 1 (Th1)
T helper 2 (Th2)
T helper 17 (Th17)
TGF- β (Transforming Growth Factor Beta)
Tumor-associated macrophages (TAMs)
Tumor microenvironment (TME)
Vascular endothelial growth factor (VEGF)
Vascular endothelial growth factor receptor (VEGFR-1)

CHAPTER 1: INTRODUCTION

Malignant solid tumors recruit the blood vessel network of the host tissue for nutrient supply, continuous growth, and gain of metastatic potential. Angiogenesis (the formation of new blood vessels), vessel cooption (the integration of existing blood vessels into the tumor vasculature), and vessel regression remodel the healthy vascular network into a tumor-specific vasculature that is, in many respects, different from the hierarchically organized arterio-venous blood vessel network of the host tissues [1].

Understanding the relationship between cancer and vascularization is crucial for the development of effective therapeutic strategies. Vasculature is formed by three main cellular processes: vasculogenesis, angiogenesis and arteriogenesis, that are the formation and remodeling into a complex vessel system that mediates the vital physiological processes including tissue oxygenation, nutrient delivery and waste removal, immune response, temperature regulation, and the maintenance of blood pressure [2].

The existence of mechanism that orchestrates the birth of new vessels, such as on the angiogenesis, plays a pivotal role which acts not only in normal physiological functions but also in pathological conditions, as cancer. While it is essential for embryonic development, wound healing, and tissue repair in normal physiological contexts, in the context of breast cancer the dysregulation of this mechanism benefits the tumor in a state of uncontrolled growth and progression, behind target of the imbalance between pro-angiogenic and anti-angiogenic factors [3]

The tumor microenvironment, an environment conducive to angiogenesis, ensures a continuous supply of nutrients and oxygen to sustain the growing tumor mass. This dysregulation creates a stimulation by hypoxia and other microenvironmental cues, which releases a cascade of signaling molecules, resulting in tumor survival and progression [1, 4]

As an alternative to traditional 2-dimensional (2D) models, the introduction of 3-dimensional (3D) models and the associated more realistic view of tumor biology has resulted in the exploitation of these models in the study of several cancer types, including breast, prostate, ovarian, lung, and colorectal cancer. 3D cultures mimicking vascularized cancer tissue allow the study of the role of the vascular component in cancer progression [5].

1.1. Breast Cancer

Breast cancer is no longer considered a single disease but is classified into several molecular subtypes based on the expression of specific hormone receptors and proteins which reflects the distinct molecular profile and clinicopathological features as part of the histological subtypes.

These molecular subtypes have been bearing the prognosis and selection of the treatment modalities [6]. The detection of variety receptors, estrogen, progesterone, human epidermal growth factor receptor 2 (HER2), delineated the beginning of molecular classification along with the Ki-67 labeling index, a marker of cell proliferation.

Breast Cancer started by being divided into four major classes, according to the molecular profiles: basal-like, normal-like, HER-2 positive and luminal-like, that is divided into luminal A and luminal B [7] [8].

The metastasis that is characteristic to this disease is one of the main reasons for the high mortality. Bones, liver, lungs, and brain are the common metastatic sites, being the bone the most common metastatic organ, while the brain is the least. Bone metastasis presents a lot of influence in the quality of life trough bone pain and tumor-induced fracture, and the decrease in the survival rate. The metastasis process involves complex steps which are the invasion, migration, adhesion, and survival of the tumour cells at the metastatic sites [9].

The theory reported in 1889 of the “seed and soil” is the representation of how the cancer metastasis develops and its dependence on the interactions between tumour cells, the “seeds”, and how the microenvironment represent the potential metastatic site, the “soil” [10, 11].

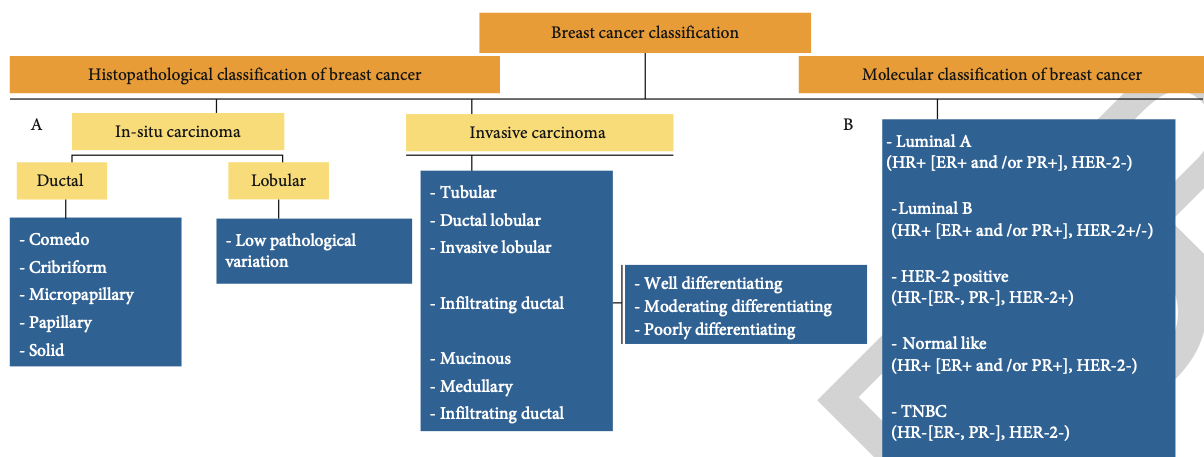


Figure 1.1 Overview of the classifications of Breast Cancer [6]

1.2 Tumor Microenvironment

Cancers can appear in any organ or body structure and consist of abnormal cell growth. The transformation of a normal cell into a cancerous cell has different types of impact, namely at the level of the immunological response. This is one of the reasons why the risk of cancer is multiplied in people whose immune system is suppressed due to several factors [12].

One of the most fundamental characteristics of cancer cells is the capacity to sustain chronic proliferation. While in normal tissues exists the control of the production and release of growth-promoting signals that ensure the homeostasis of cells and maintain the normal tissue architecture and function, cancer cells create an interference on this homeostasis with a deregulation of these signals [13].

The tumor microenvironment (TME) has been widely implicated in the connection between the tumor cells and their interaction with the surrounding environment through the circulatory and lymphatic systems to influence the development and progression of cancer [14].

Tumors are more than insular masses of proliferating cancer cells and that's the reason for the existence of a complexity on the tissues due to their composition and the interactions with one another affecting and corrupting the function and health of other cells in the body [15].

The recruitment of normal cells, which form tumor-associated stroma, and their active participation in tumorigenesis contribute to the development and expression of certain capabilities, making a stemple to understand the biology of tumors [13].

1.2.1. Extracellular matrix

The composition of the TME varies between the different tumor types, but hallmark features include immune cells, stromal cells, blood vessels, and extracellular matrix (ECM). ECM has important functions beyond the physical support that it gives to the cells, being also involved in the promotion of a tumor cell dissemination it consists of a network of macromolecules, which includes glycoproteins, collagens, and enzymes that plays a role on the influence of cell adhesion, proliferation, and communication [16, 17]

One of the key components of the ECM is growth factors implicated on the interaction between cancer cells and TME. This interaction is one reason for the influence on the migration of cancer cells which happens by altering the physical properties, composition, and structure of the ECM. The speed of cancer cell migration is determined by the adhesion gradient and ECM

concentration, cancer cells may move faster or slower depending on how concentrated the ECM is in a particular area [18].

ECM is also composed by proteins such as collagen, fibronectin, elastin, and laminin. In the case of solid tumors, it presents large amounts of ECM, being as much as 60% of the tumor mass. On this case, an excessive amount of ECM, particularly collagen, with fibroblast infiltration, leads to a what is known as desmoplasia, being associated with a poor diagnosis [19].

In a tumor environment the cancer-associated fibroblasts (CAFs) are the main producers of ECM, on the other hand, matrix metalloproteases (MMPs) are associated with the breakdown of the protein that constitute ECM, helping remodel the ECM and promoting tumor progression thereby also releasing chemokines and growth and angiogenic factors like vascular endothelial growth factor (VEGF) and fibroblast growth factor (FGFs). The integrins on the ECM also play an important role being involved on the attachment of the cells to the ECM, having an activity that is essential to the epithelial differentiation and cell development. [15, 20].

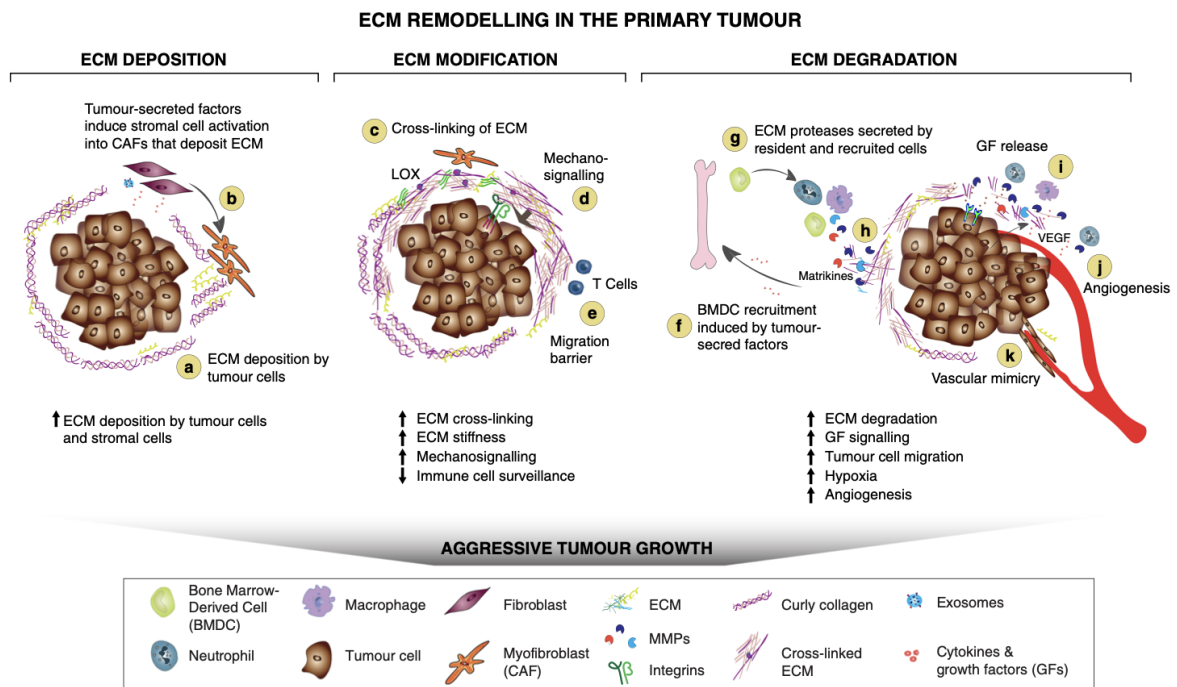


Figure 1.11 Remodeling of the ECM around a primary tumor [21]

1.2.2. Cellular Components

1.2.2.1. Stromal Cells

The cellular components are part of the tumor environment, and it consists of diverse stromal cells in addition to cancer cells. Cancer cells activate the recruitments of supporting cells from the surrounding tissue to contribute to tumor development. The composition of stromal cells can differ between tumor types, including macrophages, neutrophils, myeloid-derived suppressor cells (MDSC) and mesenchymal stem cells (MSC). After these cells start to act over the TME, it initiates the secretion of numerous factors that affect angiogenesis, proliferation, invasion, and metastasis [22].

It has been observed that hypoxia appear to exacerbate exosome production by cancer cells and promote the transition of stromal cells into CAFs [23]

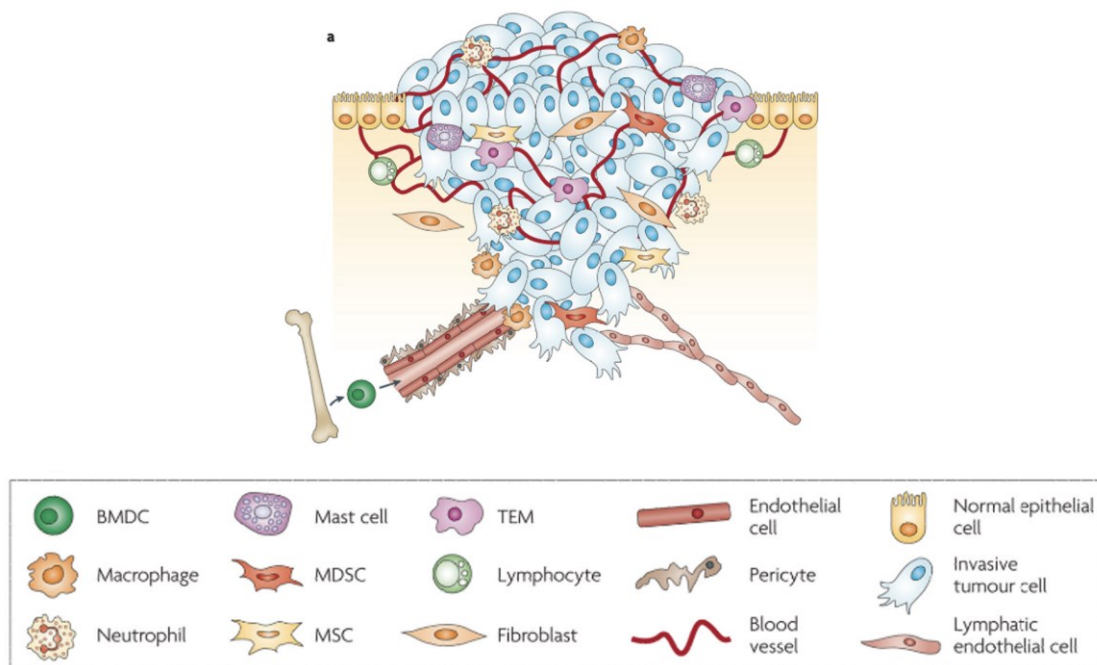


Figure 1.12 The microenvironment that surrounds cancer cells in a primary tumor [22]

1.2.2.2. Immune Cells

One of the cells groups that is part of the cellular components is the immune cells.

Tumors become infiltrated with diverse adaptive and innate immune cells that can perform both pro- and anti- tumorigenic effects. Immune cells can have two different behaviors, which is to

suppress or promote tumor growth as well as fall into two categories that represents two different approaches: adaptive immune cells and innate immune cells [24].

The exposure to specific antigens and the use of immunological memory project an immune response that is the mechanism of the adaptive immunity, on the other hand, the innate immunity represents the non-specific defense mechanism that is activated with the foreign antigen entering the body [19].

1.2.2.2.1. Adaptative Immunity

On the adaptive immunity the T-cells present receptors to recognize specific antigens. The T-cell populations are also divided according to the different roles they play. Cytotoxic T-cells (CD8⁺) have the function to detect and destroy tumor cells expressing abnormal antigens, being generally associated with a positive prognosis and suppression of angiogenesis by secreting interferon gamma (IFN- γ) [22].

CD4⁺ T-cells, which can also differentiate into various subtypes that presents other contributions, such as T helper 1 (Th1) cells that are proinflammatory with the secretion of interleukin-2 (IL-2), which gives support to CD8⁺, T helper 2 (Th2) to orchestrate an immune that supports B cells with the secretion of IL-4, IL-5, and IL-13 [21,22]. T helper 17 (Th17), on the other hand, releases IL-17A, IL-17F, IL-21, and IL-22, which promote tumor growth by acting over antimicrobial tissue inflammation. Regulatory T cells (Tregs) with the suppress of inflammation and autoimmunity can promote tumor progression in the TME. Tregs secrete IL-2, which affects natural killer (NK) cells and support cancer cell survival through growth factors and interactions with stromal cells [14].

B-cells behave to produce antibodies, present antigens, and secrete cytokines, playing significant roles in tumorigenesis: On a positive role, their functions will work in order to create interactions between T and B cells, trough the formation of ectopic lymphoid tissues within the TME, which contributes to antigen presentation, anti-tumor antibody production, and cytokine secretion (e.g., IFN- γ). Although, in some cancers, B-cells represents a negative role, trough the production of cytokines (e.g., interleukin-10 (IL-10), Transforming Growth Factor Beta (TGF- β) that promote immune suppression in macrophages, neutrophils, and cytotoxic T-cells [15, 19]. On the other hand, Natural Killer Cells drive through the bloodstream to target virally infected or tumor cells, being able to directly kill tumor cells or secrete inflammatory cytokines.

NK cells are effective against circulating tumor cells and can help block metastasis but are less efficient in the TME [25].

1.2.2.2.2. Innate Immunity

Comparatively to the innate immunity, macrophages have immune functions and release growth factors and cytokines in response to cancer cells, facilitating tumor cell proliferation, migration, and survival [14, 22]. Neutrophils represents the first line of defense against pathogens. In cancer, their role can vary between the promotion of the inflammation, in an early stage, and tumor cell apoptosis, with the release of the cytokine and reactive oxygen species [19]. In addition to the progression of the tumor, neutrophils can act to support the tumor growth with the modification of the extracellular matrix, resulting in the release of VEGF, and producing matrix metalloproteinases (MMPs), which aids in angiogenesis and tumor invasion. The connection between innate and adaptive immunity through the antigen-presenting cells is made by the Dendritic Cells (DC). It starts with the presenting of the antigens to T-cells in lymph nodes, which initialize the specific immune response, with the presence of the cytokines the change of DC function happens, which can potentially lead to immune tolerance towards tumor cells rather than an immune response [24].

1.2.2.2.3. Macrophages

As mentioned, macrophages are present in the innate immunity. They act as key players, having the functions to pathogen phagocytosis, antigen presentation, wound healing, and tissue repair. Tumor-associated macrophages (TAMs) upon polarization into M1 and M2 macrophages, are inflammatory and immune-suppressive, respectively. Tumor microenvironment through factors like hypoxia and IL-4 secretion, promotes the M2 resulting in the support of tumor growth. The presence of macrophages surrounding blood vessels in the TME, secretes VEGF-A which supports angiogenesis, leading to a poor prognosis [19, 22, 26].

TAMs due to molecules are able to lead to cell invasion and expansion with the stimulation of other cells [14].

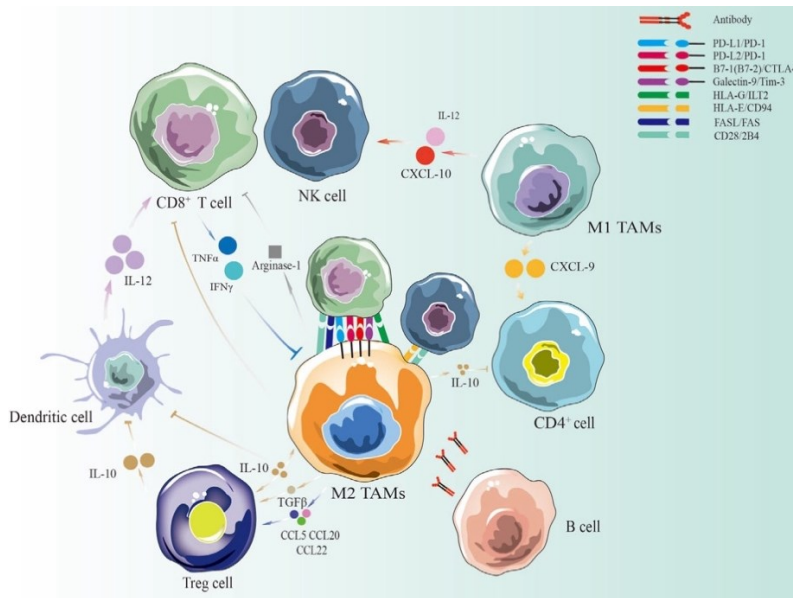


Figure 1.13 The Role of TAMs in the tumor microenvironment [27]

1.2.2.3. Cancer Associated Fibroblast: CAF

CAFs can be derived from different origins, CAFs can be formed from adipocytes, endothelial cells, pericytes, stellate cells and bone marrow derived mesenchymal stem cells. The presence of CAFs in the tumor microenvironment is associated with poor prognosis in many cancer types, despite this association, they have been shown to both promote and restrain tumorigenesis, since it came from them the production of most components, such as growth factors, cytokines and extracellular matrix, which affects the TME in four main ways: Tumor proliferation and metastasis, angiogenesis, ECM remodeling and immunosuppression [19, 28]. The conversion of fibroblasts into CAFs in the TME is influenced by cancer cells and other stroma cells which leads to the secretion of growth factors, such as hepatocyte growth factor (HGF), fibroblast growth factor (FGFs) and insulin-like growth factor 1 (IGF1) [29]. CAFs secrete TGF- β , which is essential for epithelial–mesenchymal transition (EMT) and for angiogenesis, that enables the support of tumor growth and spread, it causes the loss of epithelial cells polarity and adhesion, which allows the migration and invasion to other tissues [30]. The release of CXCL12 chemokine also promotes growth and survival of malignant cells stimulating the migration of other stromal cell types and their progenitors into the TME [23].

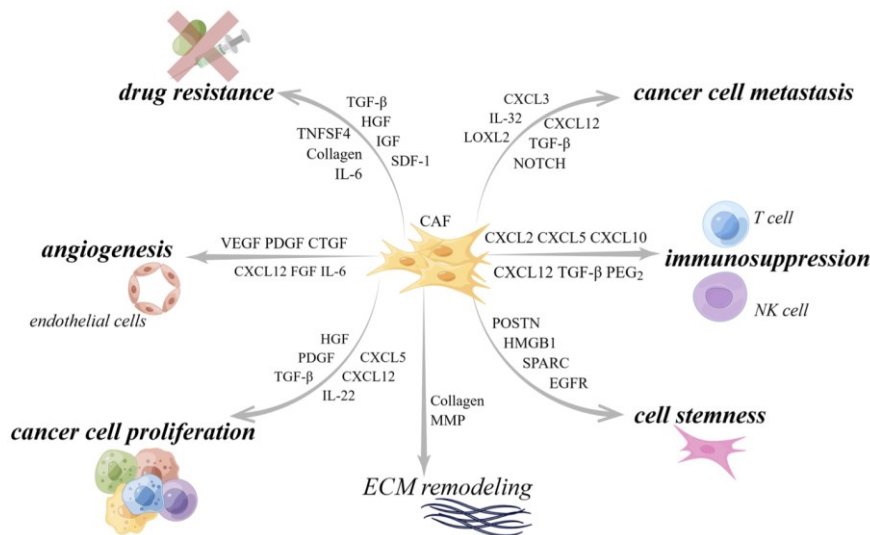


Figure 1.14 CAFs in the tumor Microenvironment [28]

1.3. Angiogenesis

Angiogenesis is a process that consists of the development of new blood vessels from existing capillaries and creates a complete, regular, and mature vascular network. The blood circulation presents a normal flow coming to the heart and passing to arteries, capillaries, and veins and coming back, due to the vascular structure formed by tight pericyte coverage and vascular endothelial cell junction. However, the mechanical stress caused by the hypertrophic tumor tissue results in a deformation of the vascularity architecture, affecting the blood circulation. Beyond the blood circulation, the lymphatic channels are also disrupted, by mechanical stress that also affects the lymphatic channels and prevents the release of excess interstitial fluid [31].

TME does not act as a silent bystander, it rather works as a promoter of cancer progression. The dynamic and reciprocal relationship that the growing of the tumor creates between cancer cells and components of the TME to give support to the survival of the cancer cells, local invasion and metastatic dissemination develops a coordination of a program to promote angiogenesis that restores oxygen/nutrient supply and remove metabolic waste [13, 32]. Tumor angiogenesis can occur in various forms, being sprouting angiogenesis the most typical consisting of the formation of new vascular branches from existing ones and then the infiltration into tumor tissue through the migration of cells and then proliferation [33]. On the other hand, angiogenesis can involve the formation of a double lumen that origins two vessels and then infiltrates into tumor tissue, the so-called intussusceptive angiogenesis, it

also happens through a process called vasculogenesis, where the recruiting of bone marrow-derived or vessel wall resident endothelial cells to create a new blood vessel happens [34, 35].

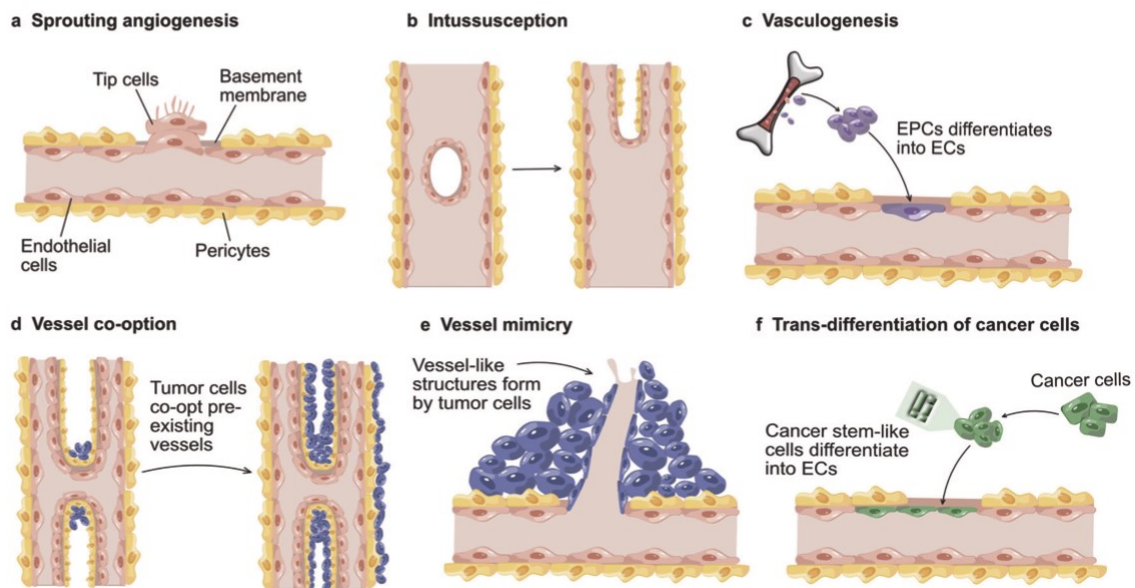


Figure 1.15 Different modes of Angiogenesis [31]

1.3.1. Mechanisms involved in angiogenesis

The altered interstitial pressure caused by the blood leakage of tumor vessels affects transportation, drug treatment is one of the examples where it is a benefit for the tumor environment such as its proliferation, adhesion, invasion, and metastasis leading to evaluation and resistance that can lead to a malignant lesion [36].

The dissemination of the tumor has been proved by some studies to be related to hypoxia. Hypoxia triggers numerous responses through hypoxia-inducible factors (HIFs) which creates stimulation over metabolism, angiogenesis, and cell division. Angiogenesis is critical in the development, progression, and metastasis of solid tumor cells, on an early phase, the tumor can remain in a dormant state due to hypoxia and low nutrients in the microenvironment, although, eventually, tumor will activate an angiogenic switch and enter in an angiogenic state initiating the recruitment of new capillaries, creating a response to the lack of oxygen and nutrients which leads to rapidly increasing tumor growth [13] [37].

These angiogenic activators involve signaling between tumor cells and numerous other cell types within the tumor microenvironment due to the production of pro-angiogenic growth

factors by the tumor cells, specific tumor cells can produce it both being able to stimulate and inhibits angiogenesis, respectively [38].

It is believed that tumors have the capability to influence the balance between angiogenesis inducers and inhibitors exerting opposing action which can be accomplished by the change of the gene transcription, that is also observed in several tumors where an increase in the levels of VEGF and/or FGFs is recorded when compared to healthy tissue. Conversely, in other tumors, the levels of endogenous inhibitors are reduced, being determinant whether or not the tumor will switch on angiogenesis [39].

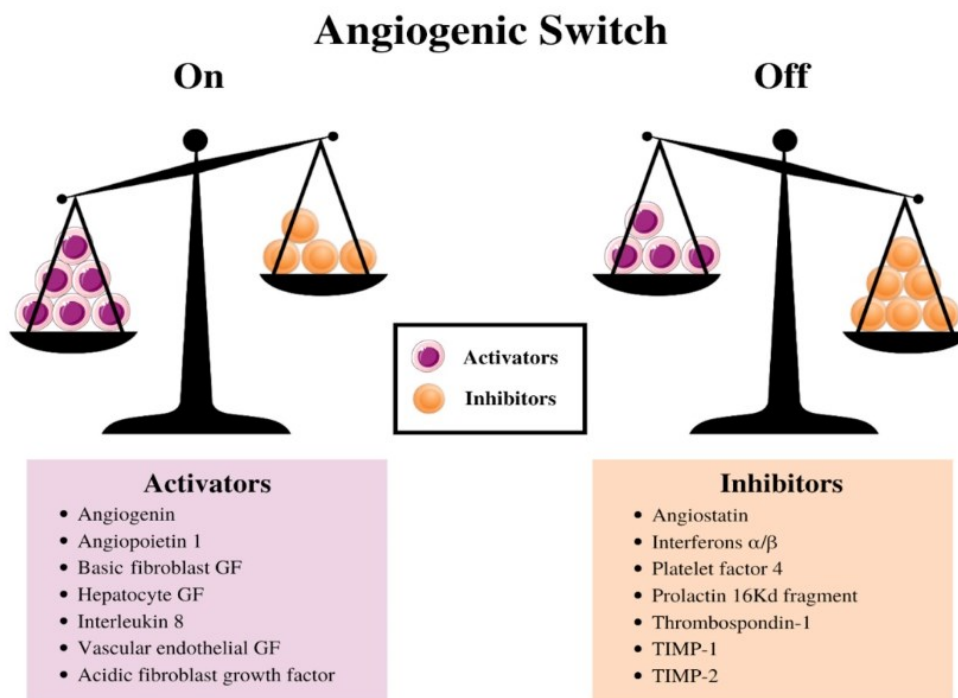


Figure 1.16 Inducers and inhibitors of Angiogenesis that affect the regular mechanism [40]

It is also present a decrease in the production of the anti-angiogenic proteins on the tumor angiogenic switch, promoting the tumor growth and metastases [41]. This especially relies on endothelial cells that express the heterodimeric transcription factor, hypoxia inducible factor 1 alpha (HIF-1 α), that was already showed to be involved on the regulation of angiogenesis, making the HIF pathway a master regulator of angiogenesis. Therefore, hypoxia and the HIF pathway are critical on the activation of the tumor cells, since they are involved in the regulation of the expression of pro-angiogenic genes [40].

1.3.2 Angiogenic Factors

The complex dynamic that influences the angiogenic system is composed with various biomolecules that balance the promotion or inhibition of angiogenesis.

Many proangiogenic factors and their receptors have been identified, even though the most emphasized proangiogenic factor is VEGF. The binding between the growth factors and their corresponding receptors, located on the endothelial cells, it initiates the activation of endothelial cells [42]

On the tumor angiogenesis VEGF presents a crucial role on the tumor environment, angiogenesis, vasculogenesis, inflammation and vascular permeability constituting the most important signaling pathways in tumor angiogenesis [43]. This mechanism happens due to the influence on endothelial cell proliferation and survival which increases the migration and invasion that acts under the permeability of existing vessels. In addition to the angiogenic action, VEGF also acts beside the vascular environment through autocrine effects on tumor cell function such as survival, migration, invasion, immune suppression, and metastasis [44, 45].

The VEGF family includes VEGF-A, VEGF-B, VEGF-C, VEGF-D and placenta growth factor (PlGF) [31]. VEGF-A presents the most important role in the regulation of angiogenesis that leads in tumor growth, proliferation, invasion, metastasis, angiogenesis, and drug resistance, VEGF-B through angiogenesis leads to the promotion of neuronal survival and cardiovascular growth, VEGF-C and VEGF- D act through the lymphangiogenesis and lymphatic metastasis which encourage tumor growth and metastasis that is mediated by VEGFR-3, blocking this pathway leads to apoptosis of lymphatic endothelial cells and disruption of the lymphatic network [46, 47]. PlGF is expressed in various tumor or non- tumor cells and is mediated by vascular endothelial growth factor receptor 1 (VEGFR-1), playing a contribution to the activation and proliferation of stromal cells including fibroblasts, macrophages, smooth muscle cells and endothelial cells [31, 47].

These angiogenic factors function not only directly with their own receptors to induce angiogenesis but also interacting with each other. An example is the competition between PlGF and VEGF-A, even though they are expressed in different cell populations, both can bind to VEGFR-1, which allows VEGF-A to interact with VEGFR-2 [47].

As previously mentioned, FGF, HGF, IGF, and TGF- β are growth factors involved in angiogenesis. In addition to these, Platelet-Derived Growth Factor (PDGF) and Epidermal Growth Factor (EGF) also play a role.

Growth Factor	Main Function
PDGF	Stimulates cell growth and differentiation and recruitment of pericyte cells which contributes to vascular maturation and cell proliferation
EGF	Promotes cell proliferation and differentiation being involved with endothelial cell which results in the secretion of various angiogenic factors, such as VEGF.
FGF	Stimulates proliferation and differentiation of endothelial cells and fibroblasts, being critical in tumor angiogenesis, related to endothelial cell migration.
HGF	Derived from mesenchymal cells and activated by extracellular protease cleavage being associated to angiogenesis and tumor proliferation,
IGF	Promotes angiogenesis by stimulating VEGF synthesis and HIF-1 α expression, linked to tumor progression and therapy resistance.
TGF- β	Induces EMT, tumor invasiveness, and up-regulates MMPs and VEGF.

Table 1 Growth factors involved in angiogenesis [3]

1.4. Role Of Endothelial Cells

As detailed above, endothelial cells are part of a thin monolayer that form the vascular endothelium and are involved in angiogenesis, specifically, through HIFs instructing them to secrete the proangiogenic factors such as, PDGF, EGF and VEGF. Beyond angiogenesis, endothelial cells promote cancer cell migration, invasion and metastasis, through the action of TGF- β inducing them to transition to a CAF [19].

The sprouting and elongation of new capillaries are critical steps where the cells proliferate to form new capillary-like sprouts, become lumenized and covered by pericytes, where the endothelial cells maintain their quiescent phenotype, which is controlled by the dynamic balance between stimulators and inhibitors of angiogenesis [48, 49].

The differentiation can occur into two types, the proliferating stalk cells, which multiply and form the body of the new blood vessel and the migrating tip cells, that form filipodia, and guide the direction of the growing sprout of the vessel [31, 50].

On the other hand, cancer cells can show a behavior similar to the endothelial cells and act like them, which is consistent in the vascular mimicry, that is associated with aggressive cancer behavior, increased risk of metastasis and poor clinical outcome [4]. Cancer cells can produce

their own blood- channel network as well as they have the ability to organize themselves into a tubular structure, which is rich in ECM and to connect to the regular blood vessels, creating a mixture of actual endothelial cells and non-endothelial cancer cells in the tumor’s vasculature through the EMT [31].

1.5.Role OF MSC

MSC present a crucial role in the interactions between tumors and the TME due to influence and participation on the tissue function once they can modulate the immune response, angiogenesis, apoptosis, oxidation level, migration, and differentiation/stimulation of surrounding cells. MSCs promote the growth of tumors with their ability to differentiate into CAFs [51].

It is due to the interaction between MSC with tumor cells directly or indirectly through the secretion of paracrine factors that MSC are associated to the enhance of the metastatic potency cancer cells, such as, breast cancer cells [52, 53].

It was observed that MSC with the exposure to conditioned media from the same MDA-MB-231 breast tumor cells were able differentiate into CAFs and become part of the tumor microenvironment, being capable of regulating epithelial- mesenchymal transition (EMT) and tumor-initiating stem cells in tumor [54, 55]

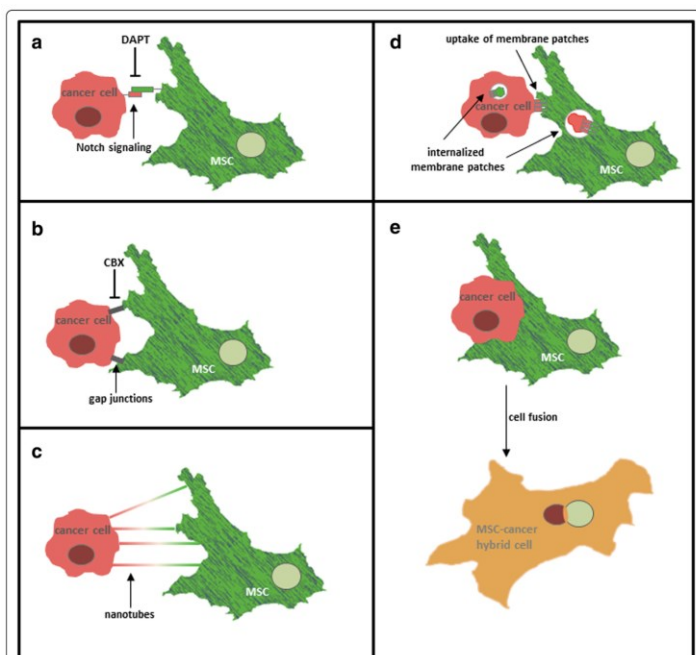


Figure 1.17 Interaction between MSC and cancer cells [56]

1.6. Theoretical background

1.6.1. 2D vs 3D models

The development of in vitro models is necessary to understand the complexity and heterogeneity of the angiogenic tumor microenvironments and the mechanisms governing the vascular intricacies. The 2D primary cell culture models of endothelial cells are the most used, which contributed to most of the knowledge on tumor endothelial cell biology. [57] Therefore, developing 3D in vitro models to mimic the complex architecture is crucial for advancing on the understanding of this topic. This model enables co-culturing endothelial cells along with other cell types increasing the knowledge on paracrine interactions of the endothelial cells. A 3D model allows control over several parameters such as cell orientation, which can, therefore, facilitate a better understanding of the tumor vascular system and associated functions [58] [59]. The formulation of biomimetic model systems involves introducing cells into compatible biomaterials while ensuring precise control of biochemical and physicochemical properties. Bioinks are a key element of any bioprinting process, in which cells are encapsulated and extruded [59].

Endothelial cells are one of the primary components of the blood vessels, and that is the reason why the assays in vitro model systems of angiogenesis highlight their proliferation, migration, and tubule formation assays. [60] As discussed above, these cells present heterogeneous functionality and different roles, the most frequently used for in vitro assays include human umbilical veins endothelial cells (HUVECs) and foreskin tissue endothelial cells (HDMECs) [59]

In this sense, 2D cell culture techniques do not fully replicate the in vivo interactions that lead to changes in cell morphology, rate and plane of cell division, and their physiological function. Currently available scaffolds make it difficult to obtain a controlled matrix that can sustain both physiological cell growth and interaction similar to that observed in vivo [61] In order to solve this gap, tumor spheroids emerge as the most common and functional scaffold-free techniques for 3D cell culture, the emergence of cell clusters starting from single cell suspensions [62]. Using various types of cells to form spheroids have been successfully used to several investigations. Using primary tumors to formulate spheroids has demonstrated the ability to modulate several molecular mechanisms that control cell proliferation and differentiation in tumors [63].

1.6.2. Cellular Spheroids models

Korff et al. 1999 developed the spheroid-based sprouting assay showing the great advantage of a 3D environment to the analyzes of the formation of a sprout [64].

Cellular spheroids can have higher cell densities. Recent studies have demonstrated better biological function obtained through 3D spheroids compared to stem cells cultured in 2D monolayer, due to easy cell-matrix interaction and direct cell-cell signaling in a 3D microenvironment [65].

Furthermore, stem cell spheroids demonstrate efficient differentiation into various tissue types, such as bone, cartilage, fat, vessels, and heart, and increased paracrine factor secretion compared to 2D stem cell culture. The production of 3D stem cell spheroids has been studied in order to increase the efficiency of osteogenic differentiation using different types of stem cells, including MSC [66].

MSC can be isolated from various tissues in an organism and have the potential to multidifferentiate into different cell lineages that are not related to their original lineages. The addition of HUVECs within MSC spheroids facilitates the formation of a pre vascularized network, promoting increased cell dissemination, viability, and proliferation [67].

The encapsulation of stem cells in hydrogels provides advantages including the improvement of cell functions in a 3D microenvironment [67, 68]. Hydrogels, such as collagen, fibrin, gelatin, silk fibroin and lysozyme, are widely used due to their excellent biocompatibility, low cytotoxicity, soft mechanical strength, enzymatic degradability in vivo, and similarity of their microenvironment to native tissues [69, 70].

1.6.3. Acoustic manipulation

3D models imply a greater complexity on multicellular tissue functions that are directed by a complex spatial orchestration of biochemical and biophysical cues in the environment. On this sense, organize cells on hydrogels to resemble the ECM physicochemical properties present a huge importance. [71].

Therefore, cell patterning is fundamental to and to recreate complex tissue organization as well as unravel biophysical mechanisms of morphogenesis. The manipulation of the position of cells to form and recreate vascular networks has been achieved through exposure to magnetic or acoustic fields, thus defining the cellular organization by the spatiotemporal distribution of the extrinsic field [72].

Specifically, the use of acoustic waves as a way of producing a pattern is an emerging technology. Through acoustic vibrations, a pressure gradient is generated in a fluid, which allows the patterning of cells that are inserted in the medium or hydrogel, thus reducing cellular damage compared to traditional bioprinting techniques. In this sense, patterning has been used to replicate biological processes such as angiogenesis. The manipulation of cell position to form and recreate vascular networks has been achieved through exposure to magnetic or acoustic fields, thus defining cellular organization by the spatiotemporal distribution of the extrinsic field [72].

Specifically, the use of acoustic waves, such as such as Faraday wave, to produce a pattern is an emerging technology. Through acoustic vibrations, a pressure gradient is generated in a fluid, which allows the patterning of cells that are inserted into the medium or hydrogel, thus reducing cellular damage compared to traditional bioprinting techniques. In this sense, patterning has been used to replicate biological processes such as angiogenesis [73].

A very clear example of this approach is the work conducted by Petta et al. 2020, using a method called Sound-Induced Morphogenesis (SIM), morphogenesis, a process based on the self-patterning of cells, was achieved through the use of acoustic surface waves to guide the formation of the structures [74, 75].

This method uses a Cymatix machine, from mimixBio, an acoustic bioprinter leveraging sound induced morphogenesis technology, and it is possible to manipulate several parameters, such as sound frequency, amplitude, and the shape of the chamber to which the cells will be exposed. In this work, it was used the standardization of spheroids made from endothelial and MSC cells that were inserted in a hydrogel, with the final formation of vascular structures.

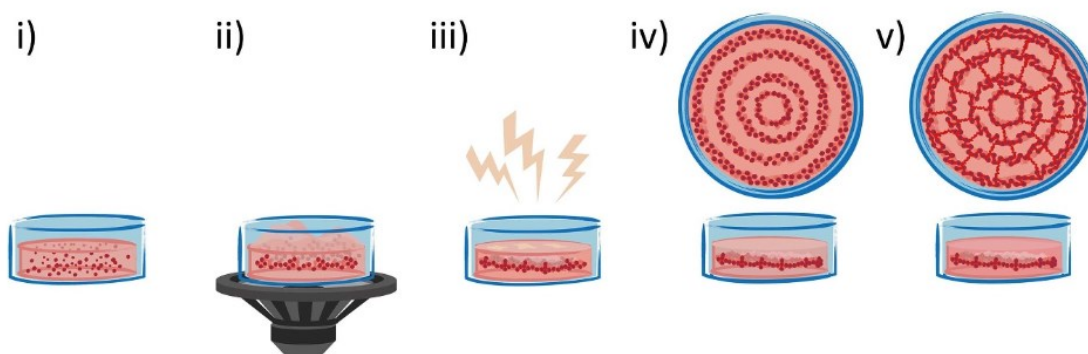


Figure 1.18 Schematic representation of the SIM process [76]

1.6.4. Tumor angiogenesis models in vitro

1.6.4.1. Sprouting angiogenesis assays

Several assays using in vitro models to study capillary formation and the various stages of angiogenesis have been performed using different methods. The use of EC cultures for capillary engineering remains an experimental challenge.

Nowak-Sliwinska et al. 2018 investigated these mechanisms through the insertion of EC on polysaccharide beads and embedding them in a hydrogel that contained fibroblasts, which contributed to promoting sprouting and the formation of lumen-containing capillaries [77].

On the other hand, Heiss et al. 2015, with the same purpose of analyzing the sprouting, embedded EC spheroids in a hydrogel composed with angiogenic factors, which gives also support to the formation of individual sprouts originating from single spheroids [78].

Both assays contributed to the study of microenvironment remodeling, and the evaluation of the sprouting formation from single spheroids.

1.6.4.2. Co-Culture Models for Angiogenesis

The use of static 3D co-culture models, where sprouting occurs as part of a more complex response involving the interactions between the tumor and the stroma, have also been performed and studied.

Namely, through Ehsan et al. 2014, whose work consisted of developing spheroids composed of tumor cells and EC, which were subsequently incorporated into a fibrin hydrogel containing fibroblasts [79].

Another approach in this sense was also undertaken by Bray et al. 2015, who investigated the interactions between tumor spheroids introduced into a compound containing EC and MSC, focusing mainly on the early stage of avascular tumor mass growth [80].

Both studies showed the projection of the sprouting to the spheroids, with the difference being the invasion of the nucleus. In fact, in the first assay, the sprouting involved all the spheroids, while in the second, it was just a projection through the surface of the spheroid.

1.6.4.3. Hydrogel Biochemical and Biophysical Properties

An important requirement for the scaffolds used on the 3D model is the capacity to support cancer cell proliferation but also angiogenesis. For this purpose, hydrogels present the ability to recapitulate the ECM [81].

The improvement of these models consists in the inclusion of other types of cells, such as immune cells, stem cells or CAF, to create a more complex tumor microenvironment. Tumor cells cultured as single cells or in spheroids require stromal cells or stromal conditioned medium since tumor cells alone do not support capillary formation [82].

Magdeldin et al. 2017 conducted a study that was focused on the ECM composition and their influence on cell proliferation and angiogenesis. Through a creation of a hydrogel where water was removed from collagen combined with tumor cells, created a dense structure that mimics a cancer mass. Then placed in another collagen hydrogel composed with laminin, a protein in the ECM, and seeded with fibroblasts, involved in the production of ECM, and EC to mimic the stromal compartment of the tumor microenvironment. The presence of laminin enhanced tumor cells to invade more aggressively, together with collagen I, regulated how cancer cells interacted with their environment and promoted both invasion and angiogenesis. It was also observed that endothelial cells, when placed in the stromal compartment, formed different types of blood vessel networks depending on the tumor cells present. [83].

1.6.4.4. Limitations

In vitro experiments to study the angiogenesis use techniques for determining cellular, biochemical, and molecular mechanisms, majority analysis of mechanisms that include endothelial migration, proliferation, sprouting, branching, differentiation, and lumen formation [84, 85]

The results that this assays present demonstrate that 3D in vitro tumor model permit their use in studying microenvironment clues of tumor progression and angiogenesis, although there is a lack in full complexity, which turns this model in a cost and time effective and easy manipulation of cell presenting an alternative tool to investigate the effect of multiple cell populations and the role of the ECM in cancer progression [83].

A limitation on these studies is that due to the lack of complexity, and once is not a in vivo model, the behavior from endothelial cells may be differently under various culture conditions.

Thus, not only is not possible to achieve the in vivo interaction that occur in vivo, the use of endothelial cells from different sources or even the number of the passages influences the results [49, 86].

1.7. Hypothesis

The goal of this work is to build up a model of vascular sprouting towards tumor spheroids formed by breast cancer cells.

For this study, 3D tumor model it will be created to form a vascular network consisting in two different layers. The bottom layer, which is the first one to be created, is composed of MSC mixed HUVECs in a form of spheroids embedded in gelatin, the chosen hydrogel. This layer will be exposed to the SIM technology to allow the formation of a vascular network, and at the same time, a pattern formation.

After the pattern is created, the enzyme, microbial transglutaminase (MTGase), which is pre-mixed with the spheroids and gelatin, allows the solidification of the layer, assuring that the pattern is maintained, and the spheroids will remain in the right position.

The top layer consists of gelatin mixed with breast cancer cells (BCC) spheroids, also pre-mixed with MTGase with the same purpose.

Building upon the theoretical framework discussed about the tumor angiogenesis being induced in a 3D model under sound induced the following hypothesis was formulated: HUVECs, when induced in a 3D model under sound stimulation, promote sprouting in response to the presence of BCC.

Chapter 2: Materials and Methods

2.1. Cultivation of SAOS-2

Sarcoma Osteogenic-2 (SAOS-2) cells were maintained in growth media consisting of Dulbecco's Modified Eagle Medium F12 medium supplemented with 10% v/v fetal bovine serum (FBS), L-Glutamine and penicillin/streptomycin 1% both, at 37°C/5% CO₂. For split the cells it was used trypsin EDTA. Passages were used between 17 and 23.

2.2. Cultivation of MDA-MB-231

MDA-MB-231 cells were maintained in growth media consisting of DMEM, high glucose, GlutaMAX™ Supplement, pyruvate with 10% v/v FBS at 37°C/5% CO₂. For split the cells it was used trypsin EDTA. Passages were used between 29 and 32.

2.3. Cultivation of HUVECS

Green fluorescent protein-expressing Human Umbilical Vein Endothelial Cells (GFP-HUVEC) were cultured in Endothelial Cell Growth Medium from PromoCell on a flask culture pre-coated with 0,5% gelatin maintained at 37 °C in a 5% CO₂ humidified atmosphere. For split it was used the DetachKit also from PromoCell. Medium was refreshed every third day and cells were used between passage 5 and 7.

2.4. Cultivation of MSC

MSC were cultured in a T-75 flask coated with 0,1% gelatin, and cultivated with *DMEM, low glucose*, GlutaMAX™ Supplement, pyruvate with 10% FBS, for split cells were detached with 3ml of TrypLE™ Express Enzyme followed by a 5 – 7 minutes incubation. Medium was changed every fourth day maintained at 37 °C in a 5% CO₂ humidified atmosphere. MSC were used between passage 4 and 5.

2.5. Culture of Spheroids

The spheroids were formed with the used of the Kugelmeiers plate 5D. First it was pipetted 1 mL of phosphate buffered saline (PBS) and centrifuged in order to avoid the formation of the bubbles. After the centrifugation and discard of PBS, 1 mL of the cell concentration was pipetted into one well and another ml of the cell culture medium add, then incubated at 37 °C and 5 % CO₂. The spheroids were always used after 24 hours, where they were pipetted up and down to a tube and centrifuged at 500 g for 5 minutes. After being centrifugated the medium was taken off and the spheroids were ready for the addition of the gelatin solution.

2.6. Preparation of the gelatin hydrogel

A 10% gelatin solution was previously prepared by dissolving gelatin type A in PBS from Sigma-Aldrich, stirred at 80°C for 2 hours. After cooling to 40°C, the pH was adjusted to 7.3 with 1 M NaOH, filtered with a 0.40 µm filter, and stored in 1 ml aliquots at 4°C. For the experiments, the gelatin was diluted with PBS to create a 2% gelatin solution, which was the desired concentration for this work.

2.7. Preparations of the inserts

The petri dishes used in this work were 60 mm petris with an inner circle insert. Although experiments with different cells were conducted, the preparation process remained consistent. After centrifuging the spheroids, the 2% diluted gelatin were added as well as the 7 units of MTGase and mixed. Then this mixture was added to the inner circle of the petri, and was immediately put on to the machine for further processing. After the patter being obtained, the petri were incubated for half a hour for the hydrogel achieved a solid form. After that step, medium was added to further incubation.

The petri where were used HUVEC, MSC and BCC, it was composed with two layers, were the top one were only added after the bottom one was solid.

Composition of the insert: SAOS - 2	
Pellet form with Spheroids, SAOS-2	
2% Gelatin: 330,8 microliters	
1.7 Units of MTGase: 9,2 µl	
6 ml SAOS-2 medium	

Table 2.1 Descripton of the constitution of the SAOS-2 insert

Composition of the insert: HUVEC:MSC and BCC	
Pellet form with Spheroids, HUVEC:MSC	Bottom layer
2% Gelatin: 330,8 microliters	
1.7 Units of MTGase: 9,2 µl	
Pellet form with Spheroids, BCC	Top layer
2% Gelatin: 330,8 microliters	
1.7 Units of MTGase: 9,2 µl	
6 ml of HUVECS medium	

Table 2.2. Descripton of the constitution of the HUVEC:MSC and BCC insert

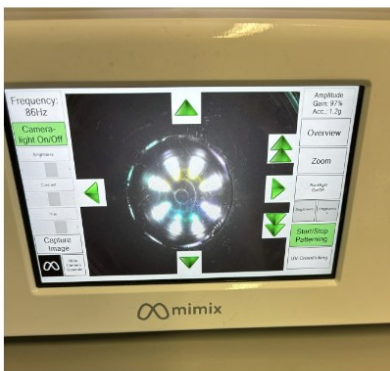
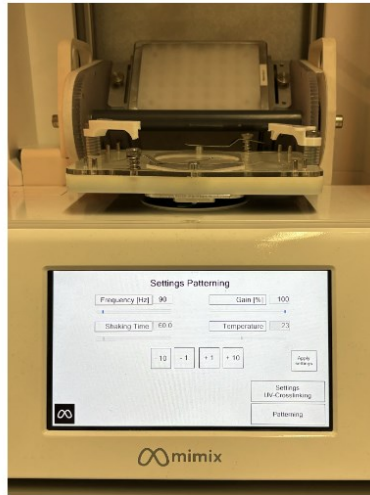
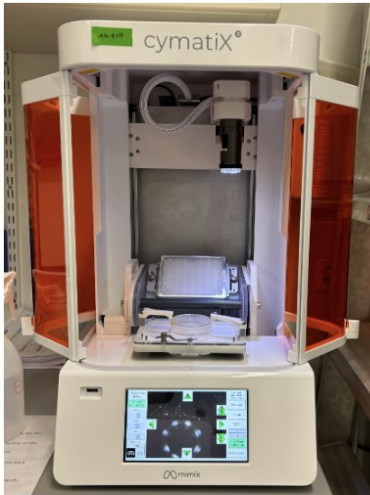


Figure 2.1 Pictures of the Cymatix, the SIM used. Show the overview of the machine. Display where the parameters of the pattern could be changed. Display showing the patterning being formed. A picture of the petri inside the machine taking by the Cymatix

2.8. Imaging

The images were captured using the Olympus IX81 fluorescence microscope.

Chapter 3: Results

3.1. Spheroids formation

3.1.1. SAOS-2

For the spheroid formation it was used one well per petri of the Kugelmeiers plate 5D which result in the formation of 750 spheroids. The number of the cells used per well it would have influence on the final size which led to the testing of different concentrations.

In the first stage, it was important to test the spheroids. Analyzing their shape and size and testing them before introducing them into the gelatin was a crucial step to ensure they were in the right conditions to rearrange themselves when exposed to SIM. These parameters were all tested with SAOS-2 cells.

In the initial trial, the formation of spheroids was tested with 0.2 million cells per milliliter, which produced spheroids with a very small size, leading to an increase in concentration. Concentrations of 1 and 1.5 million cells were tested, and both resulted in the formation of spheroids with an acceptable size, especially when using the size of spheroids used in other studies, such as a reference, which was around 100-200 μm [76].

In addition to the number of cells per well, it was also important to adjust the incubation time. Spheroids used after 24 hours of culturing were more successful than those after 48 hours. They were more visible and showed a clearer pattern in the gelatin.

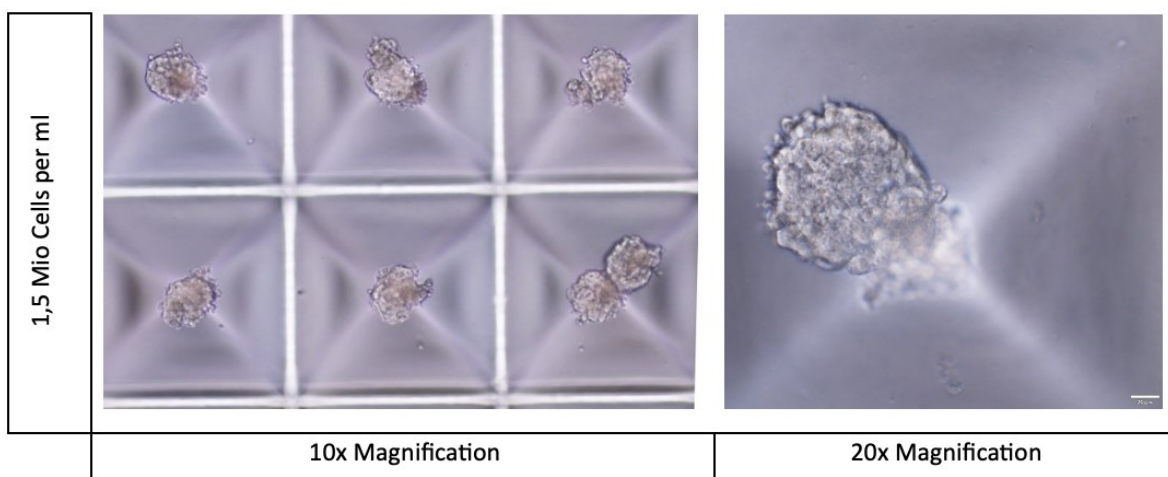


Figure 3.1. SAOS-2 Spheroids

3.1.2. MDA-MB-231

After testing with the SAOS-2 cells, which allowed achieving the parameters for spheroid formation, some adjustments were needed for the MDA-MB-231 cells due to their fast growth. Values between 0.5 and 1 million cells per milliliter were tested to understand their size after 24 hours. Since using a value of 1 million cells per milliliter resulted in a spheroid almost double the size, only 0.5 million cells per milliliter were used in the spheroids made with the BCC to maintain coherence between the spheroids in the two layers.

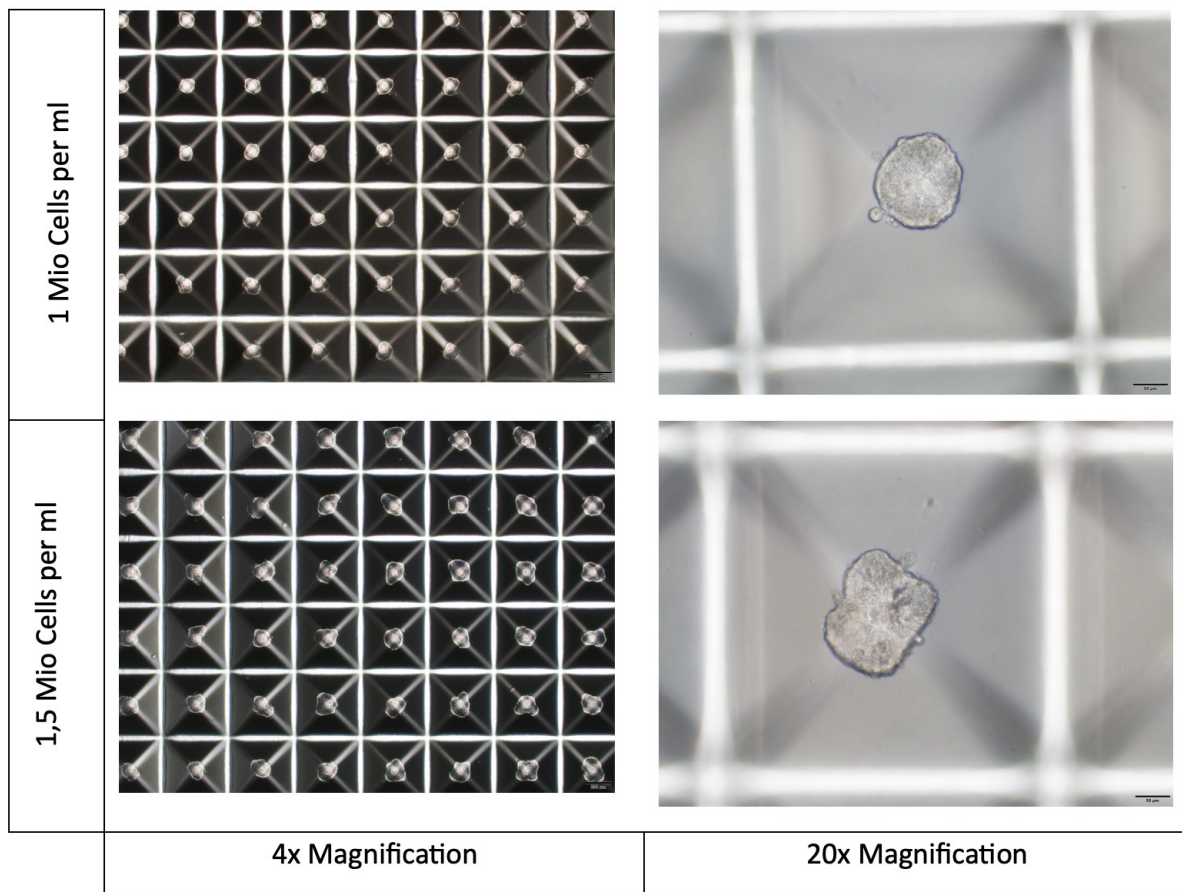


Figure 3.2 Spheroids formed with MDA-MB-231 at different concentrations

3.1.3. GFP-HUVEC: MSC (5:1)

GFP-HUVECS and MSC were tested on a proportion of 5:1 with a total of 1 Mio cells per ml, both cells were introduced on the same well and the medium added for the incubation was the medium used on the GFP-HUVECS.

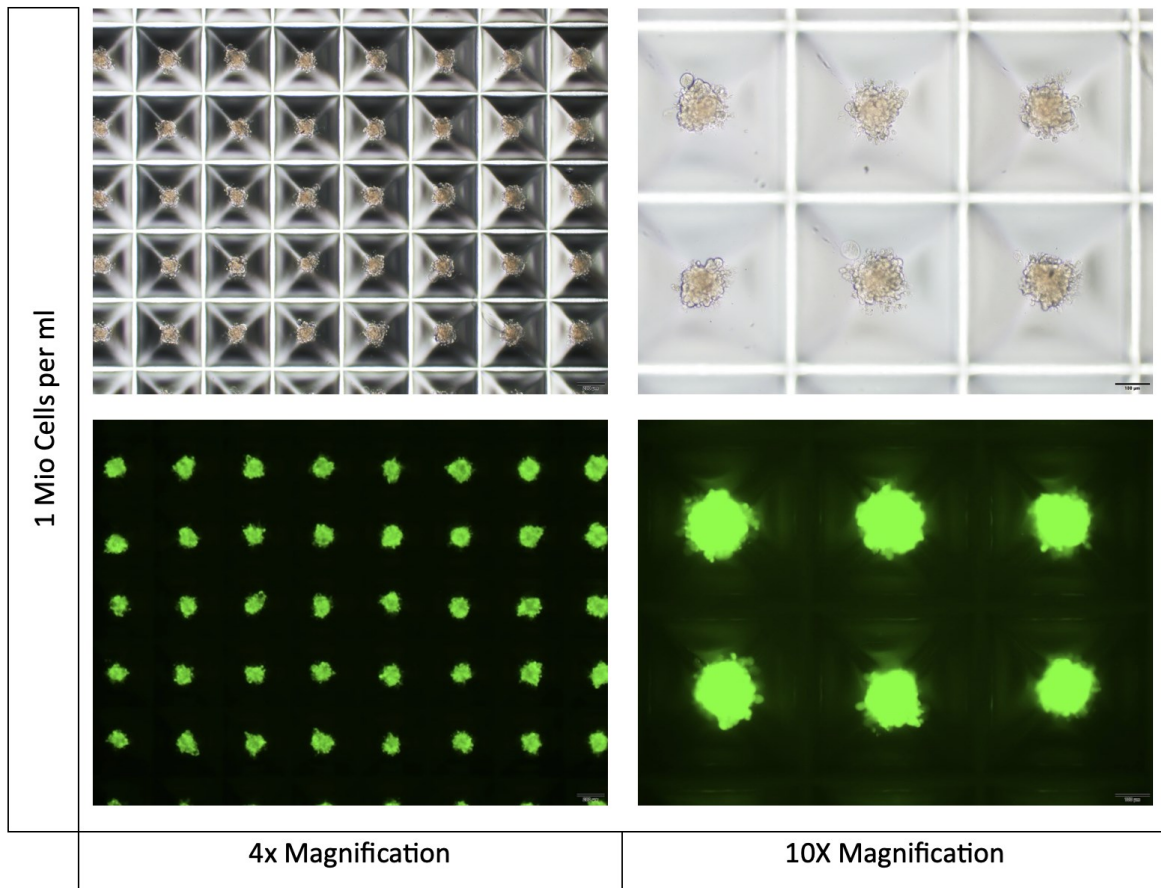


Figure 3.3 GFP-HUVEC and MSC Spheroids (5:1)

3.1.4. GFP-HUVEC:MSC (1:3)

Due to the difficulty of achieving an enough amount of GFP-HUVECS some adjustments were made, and it were tested a different proportion between HUVECS and MSC. The 1:3 with a total of 1 Mio cells.

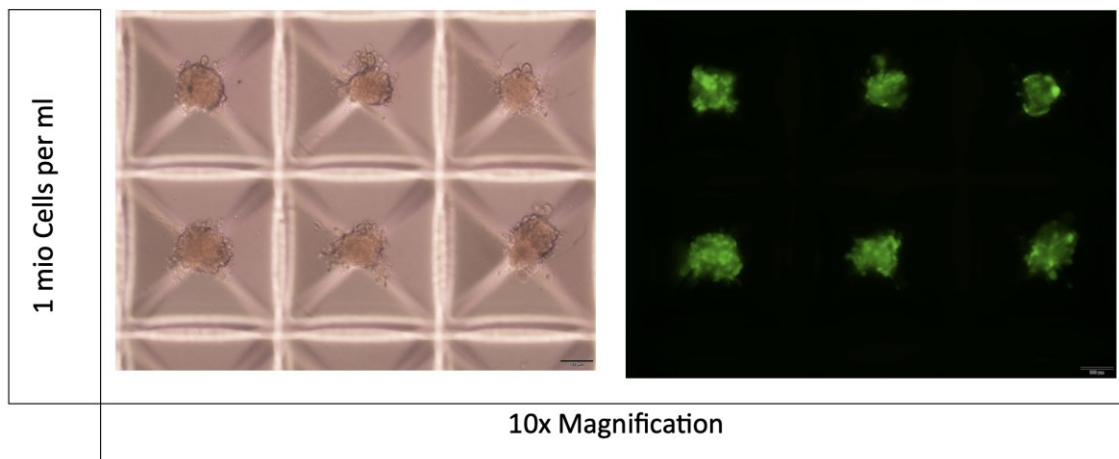


Figure 3.4 GFP-HUVEC and MSC Spheroids (1:3)

3.2. System optimization with SAOS-2

Initially, as previously mentioned, all tests were conducted using SAOS-2 spheroids. It was crucial to establish specific parameters in the SIM to achieve a pattern. The first step involved determining the optimal cell concentration for spheroid formation. It was established that a concentration ranging from 1 million to 1.5 million cells per milliliter was sufficient to produce the desired pattern.

After achieving the parameters of the machine to obtain a pattern, that was three concentric rings, it was also important to define the right number of units to use on the MTGase to be able to solidify the gelatin, after the pattern been created, in half an hour on the incubator. The spheroids were exposed to a frequency of 86 Hz and an amplitude of 98%/1.8 g.

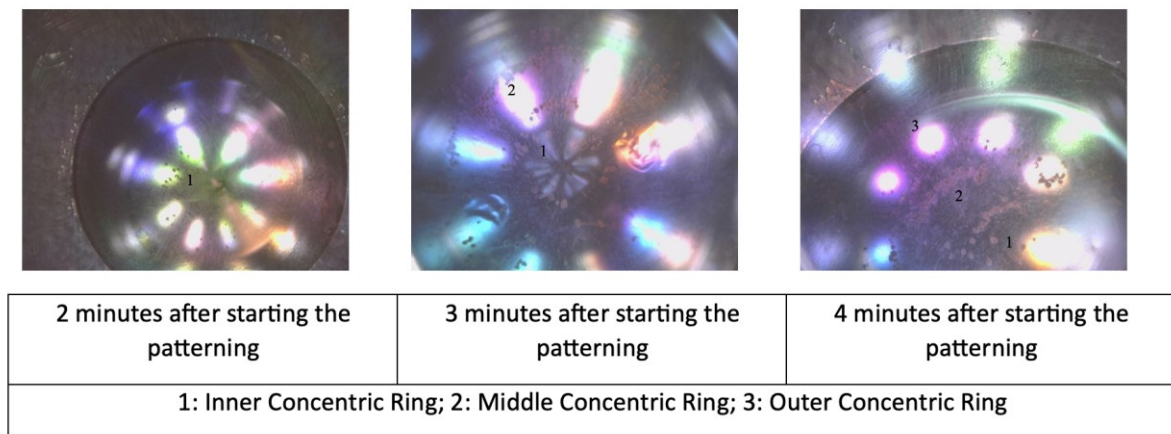


Figure 3.5. These pictures were taken with the integrated camera in the CymatiX without backlight after the machine being turned on.

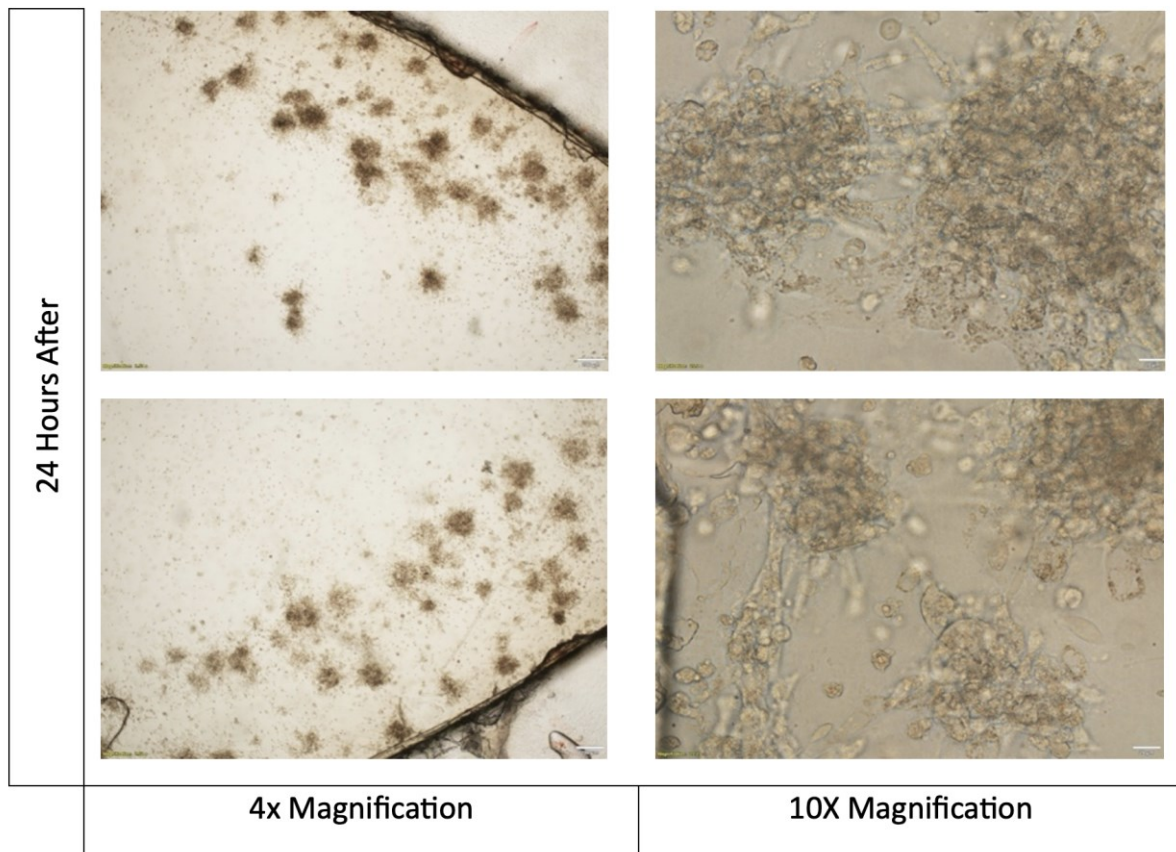


Figure 3.6. Due to the difficulty of obtaining a complete overview of the petri dish, screenshots were taken of the outer concentric ring

3.3. Observation of sprouting formation

3.3.1. 5:1 Co-Cultivation of GFP-HUVEC and MSC

A time course of over the days on the formation of the sprouts can be clearly seen under two different magnifications but also under brightfield and fluorescence images, figure 3.7 and 3.8. Immediately 1 hour after pattern formation, the spheroids showed a very rounded shape with no evidence of sprouting in both filters, their appearance is very similar to that shown in the photos taken directly from the Kugelmeiers plate, which were taken 1 hour before the pattern was made, figure 3.3.

24 hours later, there is a noticeable increase in the spheroids, where some structures may appear more spread out, but significant sprouts are still not evident. 5 days later, the photos were taken, and it is very clear the changes that have occurred with noticeable sprouts emerge from the spheroids, which is visible in both the brightfield and fluorescent images. That still can be seen

in day 6, especially on 20x the huge difference on a single spheroid compared to 24 hours later, figure 3.8.

On day 8, it is possible to observe, especially in comparison with 1 hour later, a clear evolution. Comparing these days directly, it is possible to observe a clear increase both at the level of the spheroid and at the level of the sprouts that were non-existent. All the photos to make the, almost, daily comparison was all on the same spot on the outer concentric ring, once it was not possible to achieve an overview. Although, a comparison between all the rings between day 1 and day 8 is also made, were even the outer concentric ring chosen was another spot different to the one usually used, figure 3.7.

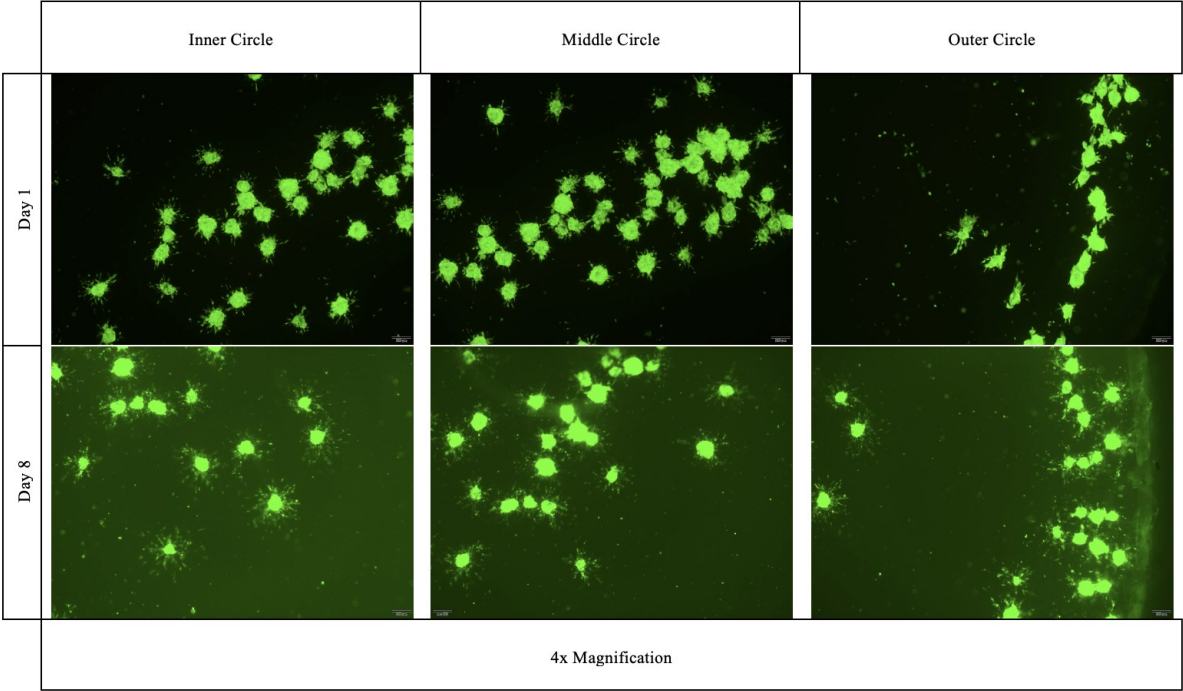


Figure 3.7 Comparison between day 1 and day 8 on the sprout formation in all the concentric rings

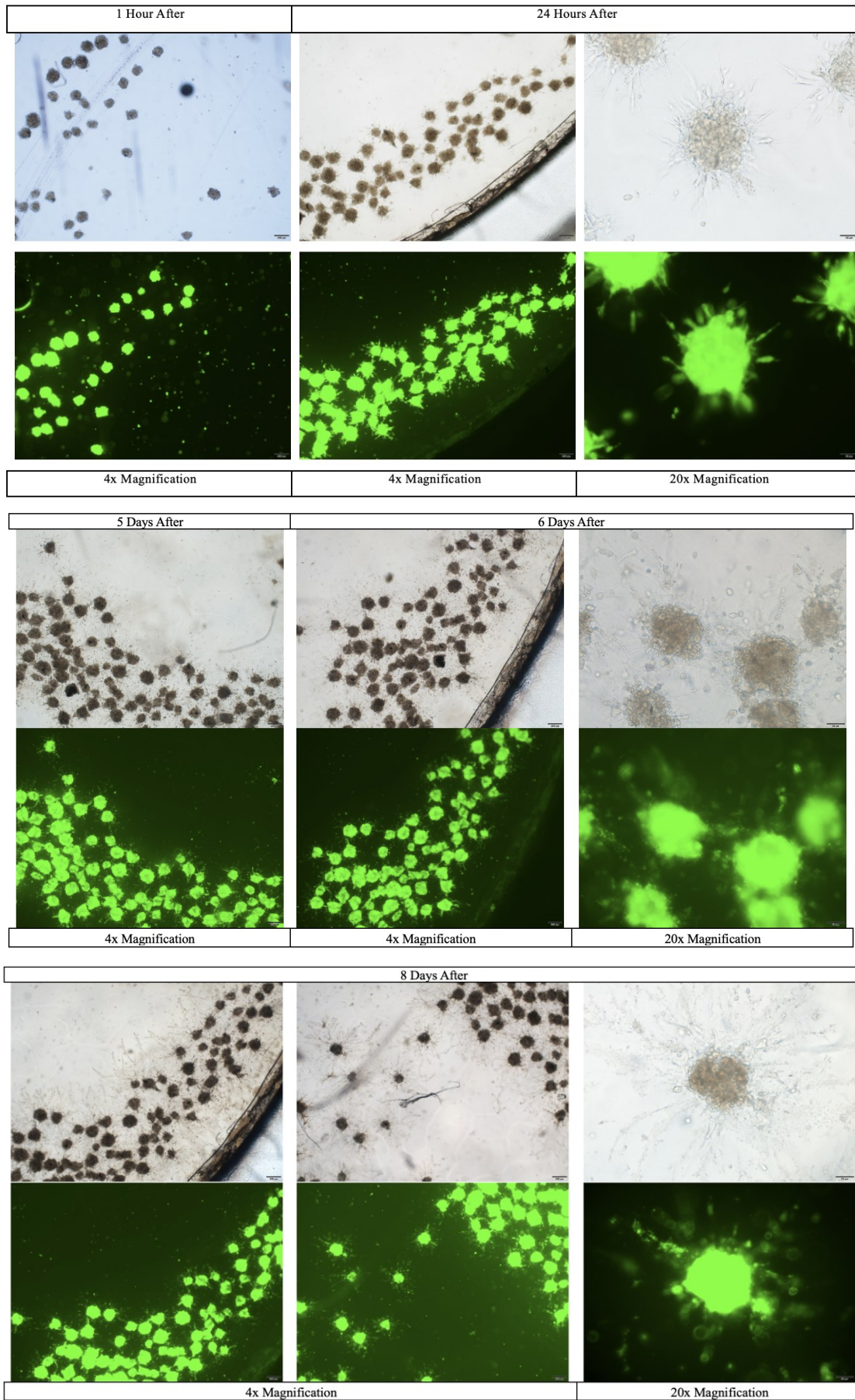


Figure 3.8 Evaluation of the sprout formation towards the days until day 8 on 5:1, HUVEC:MSC

In the second sample, it was only possible to take a photo up to day 3, since it was a sample that was obtained later. Making a direct comparison with the sample exposed to SIM, 24 hours later it presented a similar appearance. In a direct observation and based on facts, it is possible to verify the formation of sprouts, and therefore, even though there are only images up to day 3, there was in fact a response to the presence of BCC spheroid and the sprouts were formed. Based on the pictures, and in a more predictive sense, it is possible to state that the sample would possibly present the same results on day 8, and the spheroids would possibly develop in the same direction.

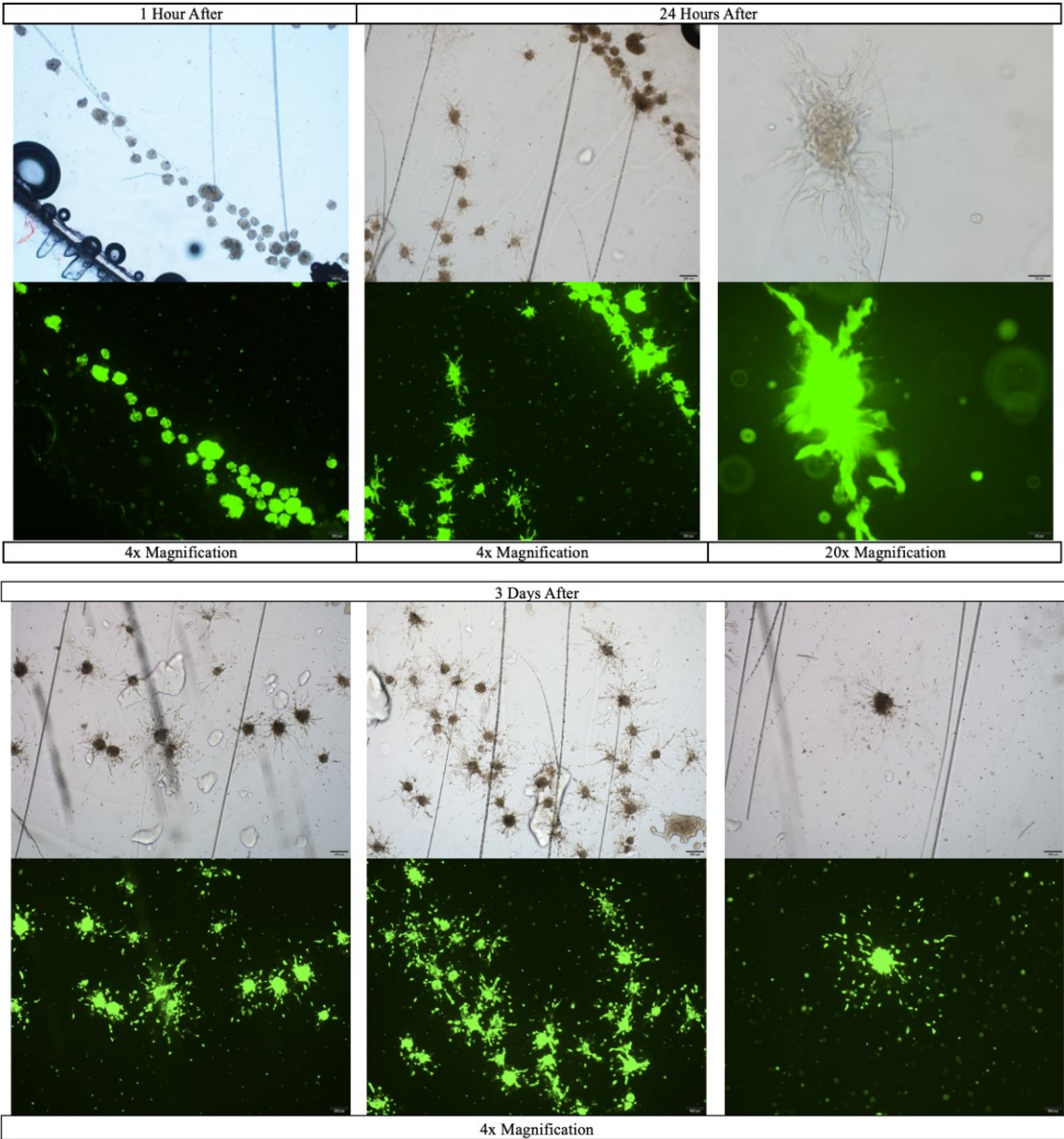


Figure 3.9 Evaluation of the sprout formation towards the days until day 3 on 5:1, HUVEC:MSC

When the brightfield images are analyzed it is possible to clearly see all the sprouts, although, in the fluorescence, there is also clear evidence of sprouting extending from the center of the

spheroids, but it is also possible to conclude that, in comparison with the brightfield images, the sprouts are not all observed at least at the focusing levels, which is justified by the projection at different layer levels within the gelatin. These conclusion fits both samples, which can also be seen in figure 3.10, even though the second sample was not analyzed until day 8, a comparison between day 6th from the 1st one and the 3rd day from the second was made, to try to reduce the time gap between them.

In fact, the projection to different layers can be conclude from both samples, although, the sprouts do not look exactly the same, the fact that there are no images from the 3rd day from the 2nd sample does not allow the direct comparison, however, it is possible to assume that the difference on the 3rd day is due to the sprouts that are beginning to form and spread, while on the 6th day, they are more developed and organized, contributing to a more mature structure.

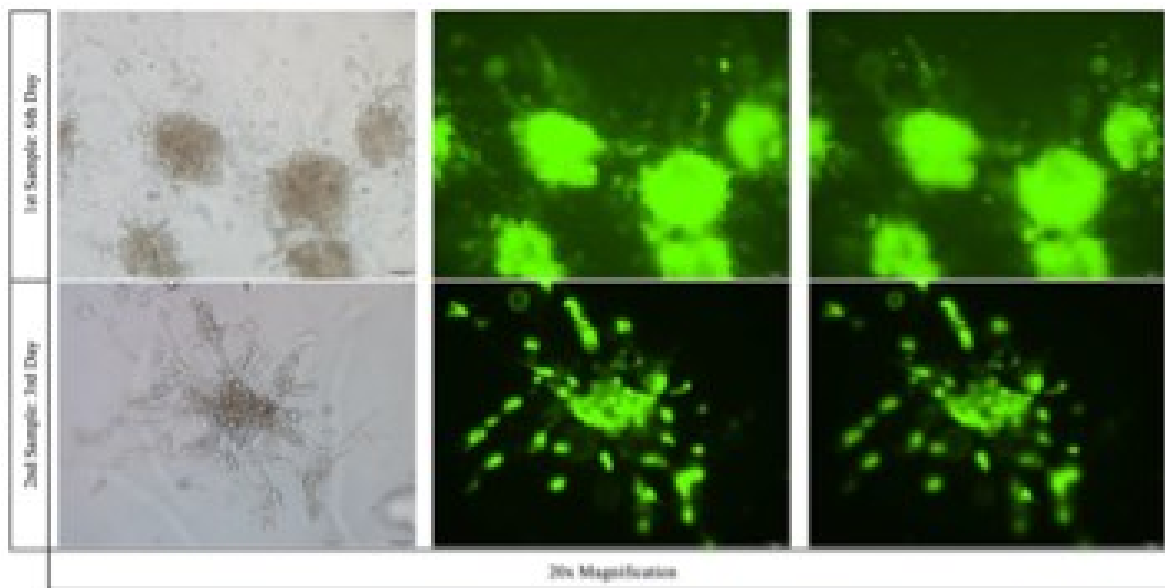


Figure 3.19 Different levels of focus on the sprouts on the samples exposed to the SIM

3.3.2. 5:1 Co-Cultivation of GFP-HUVECS and MSC without SIM

In fact, the presence of a sample not exposed to SIM is necessary, both as a control sample and to conclude whether there is a special impact on sound induction at the level of the cells. However, comparing the images obtained, effectively, not exposed to SIM, do not show a defined pattern, however, the evolution of the sprouting is very similar. The size and projection of the sprouting that emerge from the spheroids are produced in a very identical way, thus not allowing a very clear conclusion as to whether the samples used on the SIM are favored.

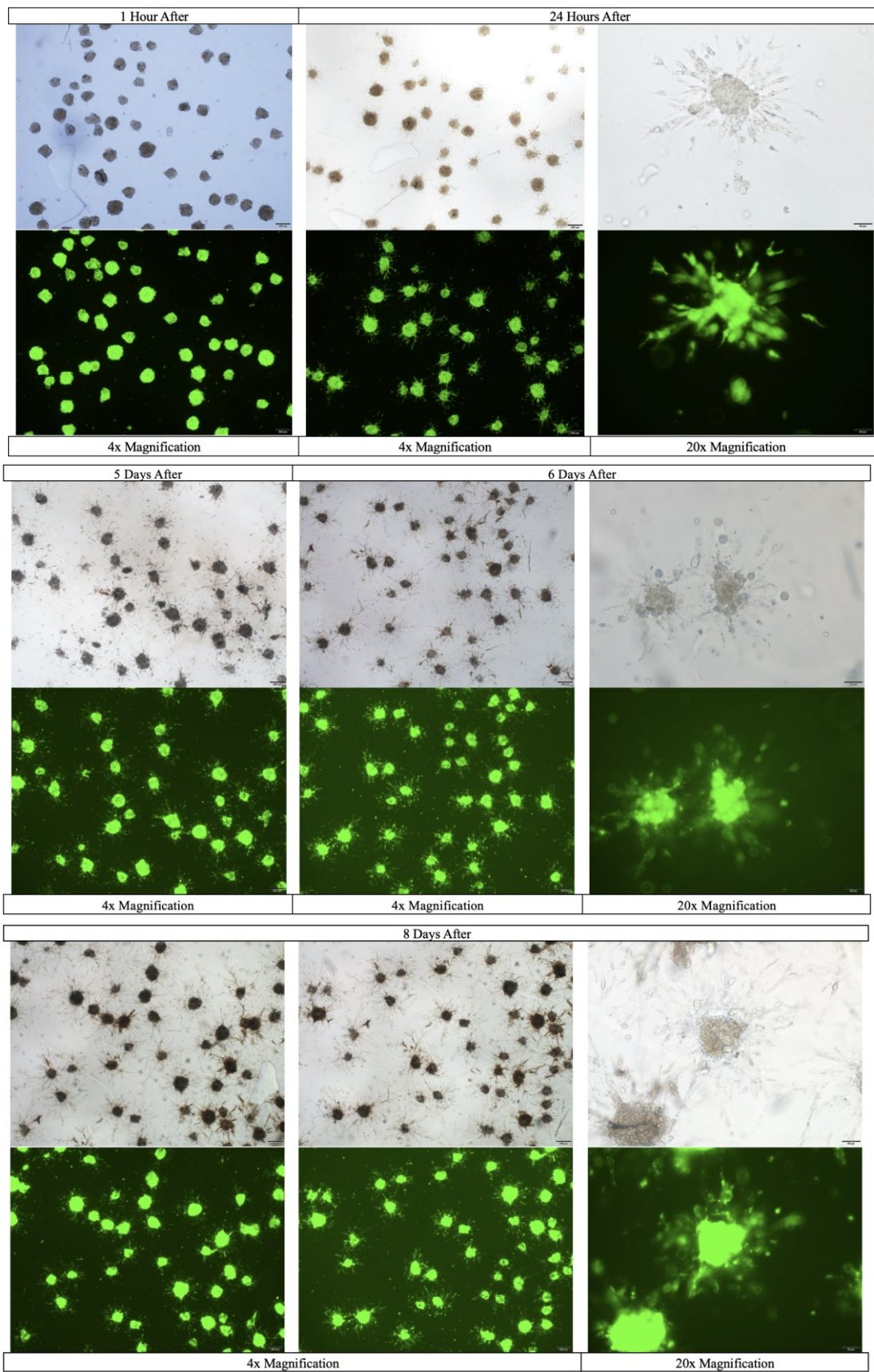


Figure 3.11 Evaluation of the sprout formation towards the days until day 8 on 5:1, HUVEC:MSC that was not exposed to the SIM

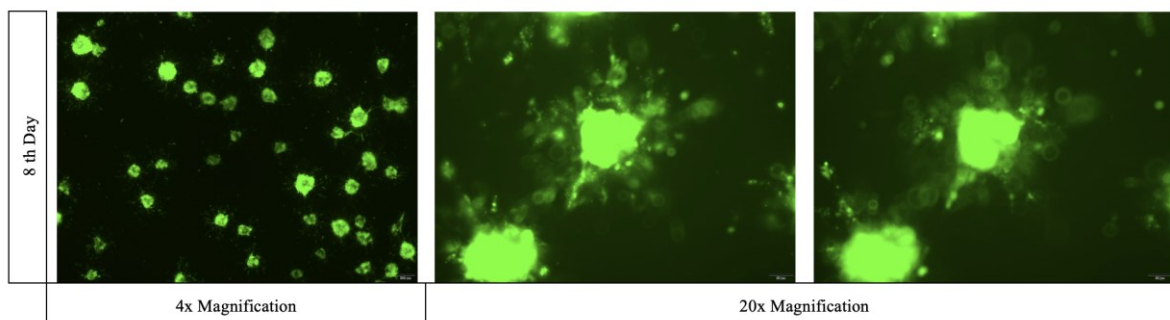


Figure 3.12 Different levels of focus on the sprouts on the sample not exposed to the SIM

3.3.3. 1:3 Co-Cultivation of GFP-HUVECS and MSC

On the 1:3 GFP-HUVECS:MSC after 24 hours it was possible to see clearly spheroids and their organization as we can see in figure 3.9. It was also possible to see on the brightfield the sprouting that were present and were projected by the spheroids, although, when with fluoresce was not possible to see that same amount what turn on immediately the possibility of a contamination with fungi, more specifically hyphae due to the presence of a long, branching, filamentous structure. In fact, a very short sprout was being projected from the spheroids as we can see in the picture of the single spheroid, which allows the possibility to believe that, in fact, sprouts would be projected eventually. Unfortunately, 48 hours later it was clear that the bigger sprouts that did not appear on the fluorescence were a result from a fungi contamination which led to the obligatoriness of discarding the petri.

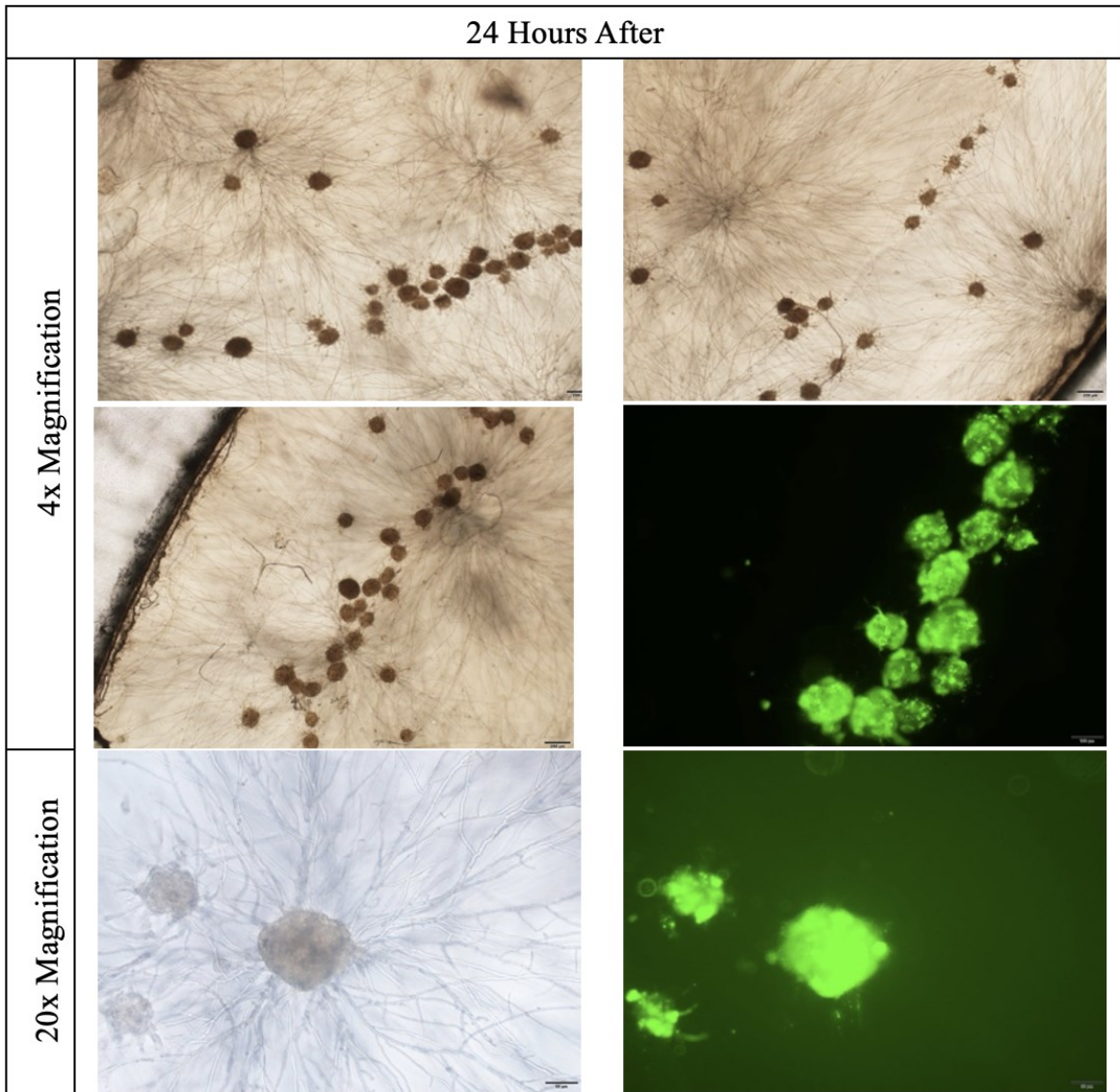


Figure 3.13. Due to the difficulty of obtaining a complete overview of the petri dish, screenshots were taken of all three concentric rings in the respective order from the inner circle to the outer one. A picture of a single spheroid was also taken

Chapter 4: Discussion

Obtaining the pattern is a demanding and inconsistent step. The fact that MTGase acts so quickly reduces a lot the time to conclude all the procedure. It is important to combined mixing it with gelatin and spheroids, the need to insert it into the Petri dish, and ensure that the entire area is covered, isolate the Petri dish with parafilm, as it is performed off the bench, and, in addition, moving it to the Cymatix, despite all of this being quick steps, impacts the time, since the enzyme itself, in a few minutes, automatically blocks the spheroids from moving and, consequently, affects the action of the machine.

Although, as shown in figures 3.1 - 3.4, the spheroids were the same size as the test spheroids, the pattern obtained was not clear and was only partial. Only half of the Petri dish showed three concentric rings, which may influence the result. The pattern obtained is due to a failure on the handling of the experience and nothing else.

In fact, the HUVEC samples, in a ratio of 1:3, contained fungal contamination, a problem that was not exactly sporadic. There were approximately three fungal contaminations during this work, which significantly affected the data collection and the time to perform the activities. These constant contaminations reduced the time dedicated to experiments with HUVECs and MSC to approximately one and a half months. During the tests with SAOS-2, two contaminations occurred that required the work to be restarted, since the incidents occurred during the parameter obtaining phase, which delayed the collection of these data. The contamination of HUVEC cells resulted in a smaller number of samples available to produce new experiments and, consequently, in obtaining results in a shorter time than expected, which affected not only the amount of data but also limited the observation of a more significant evolution. Certain steps occur outside of the bench, such as the use of the Cymatix, as previously mentioned. Additionally, the production of spheroids requires some out-of-bench work; for instance, the Kugelmeiers plate must first be centrifuged with PBS to ensure the absence of bubbles. Despite the use of parafilm to seal these materials, exposure to environmental factors remains a concern, this can also be one of the many reasons for contamination.

Regarding the samples of HUVEC:MSC in 5:1, when comparing the two samples exposed to SIM with the unexposed sample, it is not possible to highlight major differences, since the evolution of the spheroids and sprouting is similar, as shown in figures 3.7 – 3.11. However, no definitive conclusion can be drawn, since two samples were only monitored for 8 days and the

other one for only 3, and as previously mentioned, the pattern obtained was not perfect, unlike the patterns observed with SAOS-2.

Nevertheless, exposure to Cymatix results in a more uniform distribution of the spheroids in layers within the hydrogel itself. In the Brightfield images, with 20x magnification, observe several sprouting, on the other hand, on the exposure to fluorescence is not possible to have all of them visualized in a single image, being visible at different levels, as demonstrated by the different focusing perspectives, which indicates that they are inserted in different layers, figure 3.10. In this way, the fact that it is possible the observation of the sprouts, it can confirm the influence that the BCC had on promoting this angiogenic behavior. Furthermore, it is possible to observe the organization caused by Cymatix: the spheroids, and not the branches, are all visualized with the same focus level, can also be seen on figure 3.7 - 3.9 and also 3.13, once is a sample that was also exposed, which allows us to conclude that they are positioned in the same layer, as it can be seen, specially comparing to the sample that was not exposed to the SIM, even though the sprouts present the same behavior and are projected into different layer, the spheroids are also not all located on the same layer, figure 3.12.

Therefore, although the sprouting behavior in response to the presence of BCC is not distinct between samples, there is a different organization caused by the parameters used, which validates them. As observed in the SAOS-2 test cells and in different studies, frequency and gain are parameters that are validated at the standard level, thus allowing the association of values of 86Hz and 1.8G resulting in a concentric ring pattern, and it is predictable that the use of other values would result in different patterns.

Therefore, since these parameters are functional and applicable to Cymatix, changing these values could modify the pattern. As observed by *Chen et al. 2014*, where Faraday waves were also used and the cells were subjected to them, it was shown that different parameters resulted in different patterns, including the ability to change immediately when the parameters vary. This includes the change between 46Hz, 1.46G, to 60Hz, 1.90G, and the return to the initial organization within seconds after reapplying 1.46G and 46Hz [87].

This is similar to the findings of Petta et al. 2020, where even though three concentric rings were obtained, the influence of the shape of the Petri dish was also demonstrated. The difference between a square and a round one influences the pattern, even though the parameters are the same, the pattern will not be. This study, especially when compared to *Chen et al. 2014*, showed the subjectivity of the values. For instance, a set of 40Hz and 1.5G is much more like 46Hz and 1.46G than to 86Hz and 1.8G, but the pattern obtained was concentric rings instead of a more singular one [76, 87] .

These is related to the organization of the pattern, which were not a main topic of this work, once the importance was relied on the main organization and not on a specific one, once a specific one it probably would not result in a change in the result, since the function of the special organization obtained through exposure to sound induction was achieved and the spheroids were organized internally in the gelatin, as previously discussed and demonstrated in figures 3.7-3.9 and 3-10.

The same number of cells would produce the same number of spheroids. In fact, changing this value would not directly imply changes in the number of spheroids, since, as mentioned by the official website for the sale of 5D Kugelmeiers Plates, the number of cells affects the size of the spheroids. It is recommended to insert between 150 and 600 cells per well, considering that the presence of the microwells is the factor that makes it possible to produce and obtain the spheroids, with a fixed number of 750 spheroids per well. [88]. However, as a precaution, increasing this number, and consequently using more wells to obtain more spheroids, could facilitate the creation of the pattern, since a greater quantity of spheroids could enhance the formation of the three rings.

Regarding sprouting and cell behavior, as discussed in the introduction, the role of HUVECs in the tumor environment is characterized by the sprouting and elongation of new capillaries, where endothelial cells maintain their quiescent phenotype. This process is controlled by the dynamic balance between angiogenesis stimulators and inhibitors. [48, 49]. As noted, regardless of being exposed or not to SIM, this behavior was recorded and sprouts were observed at different gelatin levels, making it possible to compare them with the results obtained in other studies.

As with Heiss et al. 2015, which, despite not using BCC to stimulate HUVECS, used angiogenic factors such as VEGF, but also uses a control, and therefore, through a sample in which there is no stimulus, a direct comparison of the evolution of sprouting is established. In this sense, it is possible to observe the similarity of the results obtained in the samples obtained in this study with the samples where BCC spheroids were used. The conclusion was even obtained that the results supported the formation of tip cells that precedes the elongation of individual hair sprouts originating from single spheroids, these results being consistent with the description of the function of these cells. At the behavioral level of HUVECs, despite demonstrating the formation of hair sprouts, it also highlighted the affectation caused by the number of passages and the variability of the HUVEC donor [49].

In the same sense, it is also using HUVEC spheroids, and stimulation with angiogenic factors. Fischer et al. 2018 also obtained a result though the demonstration of a comparison between

HUVEC spheroid embedded in a collagen matrix after 24 h of sprouting under basal conditions, VEGF-A stimulation and FGF2 stimulation, and the results of the stimulated spheroids are also like those demonstrated in this study, and to the evolution under exposure to BCC. Once again, it was possible to affirm the similarity in relation to the stimulation of BCC and angiogenic factors [84].

In order to also demonstrate the role of MSC, a study was also carried out that addressed a synergistic interaction between human MSC and HUVECs in 3D spheroids loaded in collagen/fibrin hydrogels, with the addition of 50 μ L thrombin (6 unit/ mL in DPBS) and 50 μ L fibrinogen (20 mg/mL in DPBS) [84]. Thus, Heo et al. 2019 to analyze the behavior, prepared different forms such as group 1, composed with MSC suspension, group 2, MSC:HUVEC suspension, group 3, MSC-only spheroids and as group 4, MSC:HUVEC spheroids and where the 4th group showed formation of vascular network, which could be useful for supplying oxygen and nutrition to the encapsulated cells. In this sense and describing the focus on the analysis component regarding osteogenic differentiation, the results indicated that the addition of HUVECs within the MSC spheroids not only facilitated the formation of a pre-vascularized network and promoted greater dissemination, viability and cell proliferation, and that these co-culture systems increased the proliferation of HUVEC also due to the release of angiogenic factors from MSC. An aspect that is also present in the results demonstrated in this study using BCC [58].

CHAPTER 5: Conclusions and Future Prospects

As a final assessment, it is possible to state that the presence of BCC and, therefore, the tumor environment created, where HUVECs and MSC were inserted, promoted the production and projection of sprouting. Regarding the submission to sound induction, this is a topic in which it is not possible to establish any advantage at the angiogenic level, and, therefore, it is not possible to state that angiogenesis occurred exclusively when exposed to the sound waves. However, it is possible to state that there is a spatial organization of the spheroids resulting in a more structured spatial organization of sprouting.

In fact, the results obtained allow conclusions to be drawn, but also indicate improvements that can be made. Relating two very important topics, the action of MTGase and the contaminations suffered, the complete execution of the process on the bench, including the introduction of Cymatix on the bench, would contribute positively to these two points: the reduction of the time after addition of the enzyme and the reduction of the risk of contamination, even if there is a need for off-bench production of the spheroids, due to the production method.

Regarding SIM, the optimization of the procedure would be extremely beneficial. Repeating the process, using samples whose pattern is not incomplete or inconsistent, is important. Even if the obtained parameters were validated, testing new values of gain and frequency, and therefore obtaining new patterns, would also be an interesting approach, as would increasing the number of samples.

Due to the lack of cells, it was not possible, but testing different sample conditions is interesting. One of the ideas would be, once HUVEC culture medium was added, to test the addition of a combination of HUVEC medium with BCC medium, to analyze whether there would be greater potentiation. In this sense, incorporating BCCs in the form of spheroids was a beneficial choice due to their aggregation into clusters, which would make sense, namely by mimicking the natural cellular organization found in tissues. However, incorporating MDA-MB-231 in the top layer, or even another type of breast cancer cells such as MCF-7, or a combination of two types, as spheroids, as is the case of HUVECS and MSC that are combined, or even in the form of cells, and not just in the form of spheroids, are very interesting approaches for future testing.

It would also be beneficial to replicate this study with a slight adjustment in other parameters, namely in the number of spheroids, to enhance the existing pattern and circumvent the possibility of incomplete formation, in addition to a longer temporal analysis. A longer period could allow the visualization of more relevant aspects, such as a greater evolution of sprouting, namely the formation of vascular structures, especially with higher magnification images.

Bibliography

1. Rieger, H. and M. Welter, *Integrative models of vascular remodeling during tumor growth*. Wiley Interdiscip Rev Syst Biol Med, 2015. **7**(3): p. 113-29.
2. Patel-Hett, S. and P.A. D'Amore, *Signal transduction in vasculogenesis and developmental angiogenesis*. Int J Dev Biol, 2011. **55**(4-5): p. 353-63.
3. Liu, Z.-L., et al., *Angiogenic signaling pathways and anti-angiogenic therapy for cancer*. Signal Transduction and Targeted Therapy, 2023. **8**(1): p. 198.
4. Teleanu, R.I., et al., *Tumor Angiogenesis and Anti-Angiogenic Strategies for Cancer Treatment*. J Clin Med, 2019. **9**(1).
5. Chwalek, K., L.J. Bray, and C. Werner, *Tissue-engineered 3D tumor angiogenesis models: Potential technologies for anti-cancer drug discovery*. Advanced Drug Delivery Reviews, 2014. **79-80**: p. 30-39.
6. Kashyap, D., et al., *Global Increase in Breast Cancer Incidence: Risk Factors and Preventive Measures*. Biomed Res Int, 2022. **2022**: p. 9605439.
7. Goldhirsch, A., et al., *Strategies for subtypes--dealing with the diversity of breast cancer: highlights of the St. Gallen International Expert Consensus on the Primary Therapy of Early Breast Cancer 2011*. Ann Oncol, 2011. **22**(8): p. 1736-47.
8. Al-Thoubaity, F.K., *Molecular classification of breast cancer: A retrospective cohort study*. Ann Med Surg (Lond), 2020. **49**: p. 44-48.
9. Smolarz, B., A.Z. Nowak, and H. Romanowicz, *Breast Cancer-Epidemiology, Classification, Pathogenesis and Treatment (Review of Literature)*. Cancers (Basel), 2022. **14**(10).
10. Shao, H. and P. Varamini, *Breast Cancer Bone Metastasis: A Narrative Review of Emerging Targeted Drug Delivery Systems*. Cells, 2022. **11**(3).
11. Peinado, H., et al., *Pre-metastatic niches: organ-specific homes for metastases*. Nat Rev Cancer, 2017. **17**(5): p. 302-317.
12. Roy, P.S. and B.J. Saikia, *Cancer and cure: A critical analysis*. Indian J Cancer, 2016. **53**(3): p. 441-442.
13. Hanahan, D. and R.A. Weinberg, *Hallmarks of cancer: the next generation*. Cell, 2011. **144**(5): p. 646-74.
14. Arneth, B., *Tumor Microenvironment*. Medicina (Kaunas), 2019. **56**(1).
15. Balkwill, F.R., M. Capasso, and T. Hagemann, *The tumor microenvironment at a glance*. J Cell Sci, 2012. **125**(Pt 23): p. 5591-6.
16. Feig, C., et al., *Targeting CXCL12 from FAP-expressing carcinoma-associated fibroblasts synergizes with anti-PD-L1 immunotherapy in pancreatic cancer*. Proceedings of the National Academy of Sciences, 2013. **110**(50): p. 20212-20217.
17. Anderson, B.O., et al., *Optimisation of breast cancer management in low-resource and middle-resource countries: executive summary of the Breast Health Global Initiative consensus, 2010*. The Lancet Oncology, 2011. **12**(4): p. 387-398.
18. Tlsty, T.D. and L.M. Coussens, *Tumor stroma and regulation of cancer development*. Annu Rev Pathol, 2006. **1**: p. 119-50.
19. Anderson, N.M. and M.C. Simon, *The tumor microenvironment*. Curr Biol, 2020. **30**(16): p. R921-r925.
20. Lerner, I., et al., *Heparanase powers a chronic inflammatory circuit that promotes colitis-associated tumorigenesis in mice*. The Journal of Clinical Investigation, 2011. **121**(5): p. 1709-1721.
21. Winkler, J., et al., *Concepts of extracellular matrix remodelling in tumour progression and metastasis*. Nat Commun, 2020. **11**(1): p. 5120.
22. Joyce, J.A. and J.W. Pollard, *Microenvironmental regulation of metastasis*. Nat Rev Cancer, 2009. **9**(4): p. 239-52.

23. Orimo, A., et al., *Stromal fibroblasts present in invasive human breast carcinomas promote tumor growth and angiogenesis through elevated SDF-1/CXCL12 secretion*. Cell, 2005. **121**(3): p. 335-48.
24. Hinshaw, D.C. and L.A. Shevde, *The Tumor Microenvironment Innately Modulates Cancer Progression*. Cancer Res, 2019. **79**(18): p. 4557-4566.
25. Vivier, E., et al., *Targeting natural killer cells and natural killer T cells in cancer*. Nature Reviews Immunology, 2012. **12**(4): p. 239-252.
26. Wang, S.-C., et al., *Tumor-secreted SDF-1 promotes glioma invasiveness and TAM tropism toward hypoxia in a murine astrocytoma model*. Laboratory Investigation, 2012. **92**(1): p. 151-162.
27. Cheng, K., et al., *Tumor-associated macrophages in liver cancer: From mechanisms to therapy*. Cancer Commun (Lond), 2022. **42**(11): p. 1112-1140.
28. Zhang, H., et al., *Define cancer-associated fibroblasts (CAFs) in the tumor microenvironment: new opportunities in cancer immunotherapy and advances in clinical trials*. Mol Cancer, 2023. **22**(1): p. 159.
29. Spaeth, E.L., et al., *Mesenchymal stem cell transition to tumor-associated fibroblasts contributes to fibrovascular network expansion and tumor progression*. PLoS One, 2009. **4**(4): p. e4992.
30. Erez, N., et al., *Cancer-Associated Fibroblasts Are Activated in Incipient Neoplasia to Orchestrate Tumor-Promoting Inflammation in an NF-kappaB-Dependent Manner*. Cancer Cell, 2010. **17**(2): p. 135-47.
31. Liu, Z.L., et al., *Angiogenic signaling pathways and anti-angiogenic therapy for cancer*. Signal Transduct Target Ther, 2023. **8**(1): p. 198.
32. Chen, F., et al., *New horizons in tumor microenvironment biology: challenges and opportunities*. BMC Medicine, 2015. **13**(1): p. 45.
33. Hillen, F. and A.W. Griffioen, *Tumour vascularization: sprouting angiogenesis and beyond*. Cancer Metastasis Rev, 2007. **26**(3-4): p. 489-502.
34. Gianni-Barrera, R., et al., *Split for the cure: VEGF, PDGF-BB and intussusception in therapeutic angiogenesis*. Biochem Soc Trans, 2014. **42**(6): p. 1637-42.
35. Ratajska, A., et al., *Vasculogenesis and Its Cellular Therapeutic Applications*. Cells Tissues Organs, 2017. **203**(3): p. 141-152.
36. Milosevic, M., et al., *The human tumor microenvironment: invasive (needle) measurement of oxygen and interstitial fluid pressure*. Semin Radiat Oncol, 2004. **14**(3): p. 249-58.
37. Hanahan, D. and J. Folkman, *Patterns and emerging mechanisms of the angiogenic switch during tumorigenesis*. Cell, 1996. **86**(3): p. 353-64.
38. Carmeliet, P., *Angiogenesis in life, disease and medicine*. Nature, 2005. **438**(7070): p. 932-6.
39. Volpert, O.V., K.M. Dameron, and N. Bouck, *Sequential development of an angiogenic phenotype by human fibroblasts progressing to tumorigenicity*. Oncogene, 1997. **14**(12): p. 1495-502.
40. Madu, C.O., et al., *Angiogenesis in Breast Cancer Progression, Diagnosis, and Treatment*. J Cancer, 2020. **11**(15): p. 4474-4494.
41. Good, D.J., et al., *A tumor suppressor-dependent inhibitor of angiogenesis is immunologically and functionally indistinguishable from a fragment of thrombospondin*. Proc Natl Acad Sci U S A, 1990. **87**(17): p. 6624-8.
42. Landgren, E., et al., *Placenta growth factor stimulates MAP kinase and mitogenicity but not phospholipase C-gamma and migration of endothelial cells expressing Flt 1*. Oncogene, 1998. **16**(3): p. 359-67.
43. Hicklin, D.J. and L.M. Ellis, *Role of the vascular endothelial growth factor pathway in tumor growth and angiogenesis*. J Clin Oncol, 2005. **23**(5): p. 1011-27.
44. Lee, J.C., et al., *Prognostic value of vascular endothelial growth factor expression in colorectal cancer patients*. Eur J Cancer, 2000. **36**(6): p. 748-53.

45. Kaplan, R.N., et al., *VEGFR1-positive haematopoietic bone marrow progenitors initiate the pre-metastatic niche*. *Nature*, 2005. **438**(7069): p. 820-7.
46. Su, J.L., et al., *The role of the VEGF-C/VEGFR-3 axis in cancer progression*. *Br J Cancer*, 2007. **96**(4): p. 541-5.
47. Niu, G. and X. Chen, *Vascular endothelial growth factor as an anti-angiogenic target for cancer therapy*. *Curr Drug Targets*, 2010. **11**(8): p. 1000-17.
48. Iruela-Arispe, M.L. and H.F. Dvorak, *Angiogenesis: a dynamic balance of stimulators and inhibitors*. *Thromb Haemost*, 1997. **78**(1): p. 672-7.
49. Heiss, M., et al., *Endothelial cell spheroids as a versatile tool to study angiogenesis in vitro*. *Faseb j*, 2015. **29**(7): p. 3076-84.
50. Gerhardt, H., et al., *VEGF guides angiogenic sprouting utilizing endothelial tip cell filopodia*. *J Cell Biol*, 2003. **161**(6): p. 1163-77.
51. Friedenstein, A.J., R.K. Chailakhjan, and K.S. Lalykina, *The development of fibroblast colonies in monolayer cultures of guinea-pig bone marrow and spleen cells*. *Cell Tissue Kinet*, 1970. **3**(4): p. 393-403.
52. Vonk, L.A., et al., *Autologous, allogeneic, induced pluripotent stem cell or a combination stem cell therapy? Where are we headed in cartilage repair and why: a concise review*. *Stem Cell Res Ther*, 2015. **6**(1): p. 94.
53. Caplan, A.I. and D. Correa, *The MSC: an injury drugstore*. *Cell Stem Cell*, 2011. **9**(1): p. 11-5.
54. Polyak, K. and R.A. Weinberg, *Transitions between epithelial and mesenchymal states: acquisition of malignant and stem cell traits*. *Nat Rev Cancer*, 2009. **9**(4): p. 265-73.
55. Mishra, P.J., et al., *Carcinoma-associated fibroblast-like differentiation of human mesenchymal stem cells*. *Cancer Res*, 2008. **68**(11): p. 4331-9.
56. Melzer, C., Y. Yang, and R. Hass, *Interaction of MSC with tumor cells*. *Cell Commun Signal*, 2016. **14**(1): p. 20.
57. Bhattacharya, A., et al., *Exploring the interaction between extracellular matrix components in a 3D organoid disease model to replicate the pathophysiology of breast cancer*. *J Exp Clin Cancer Res*, 2023. **42**(1): p. 343.
58. Heo, D.N., M. Hospodiuk, and I.T. Ozbolat, *Synergistic interplay between human MSCs and HUVECs in 3D spheroids laden in collagen/fibrin hydrogels for bone tissue engineering*. *Acta Biomater*, 2019. **95**: p. 348-356.
59. Bhat, S.M., et al., *3D tumor angiogenesis models: recent advances and challenges*. *J Cancer Res Clin Oncol*, 2021. **147**(12): p. 3477-3494.
60. Castro, P.R., et al., *Cellular and Molecular Heterogeneity Associated with Vessel Formation Processes*. *Biomed Res Int*, 2018. **2018**: p. 6740408.
61. Cunha, C., et al., *3D culture of adult mouse neural stem cells within functionalized self-assembling peptide scaffolds*. *Int J Nanomedicine*, 2011. **6**: p. 943-55.
62. Zhao, X., et al., *Global gene expression profiling confirms the molecular fidelity of primary tumor-based orthotopic xenograft mouse models of medulloblastoma*. *Neuro-Oncology*, 2012. **14**(5): p. 574-583.
63. Mueller-Klieser, W., *Three-dimensional cell cultures: from molecular mechanisms to clinical applications*. *Am J Physiol*, 1997. **273**(4): p. C1109-23.
64. Korff, T. and H.G. Augustin, *Tensional forces in fibrillar extracellular matrices control directional capillary sprouting*. *J Cell Sci*, 1999. **112 (Pt 19)**: p. 3249-58.
65. Fennema, E., et al., *Spheroid culture as a tool for creating 3D complex tissues*. *Trends in Biotechnology*, 2013. **31**(2): p. 108-115.
66. Jiang, B., et al., *Generation of cardiac spheres from primate pluripotent stem cells in a small molecule-based 3D system*. *Biomaterials*, 2015. **65**: p. 103-114.
67. Nicodemus, G.D. and S.J. Bryant, *Cell Encapsulation in Biodegradable Hydrogels for Tissue Engineering Applications*. *Tissue Engineering Part B: Reviews*, 2008. **14**(2): p. 149-165.

68. Hsu, T.W., et al., *Transplantation of 3D MSC/HUVEC spheroids with neuroprotective and proangiogenic potentials ameliorates ischemic stroke brain injury*. *Biomaterials*, 2021. **272**: p. 120765.
69. Pal, K., A.K. Banthia, and D.K. Majumdar, *Hydrogels for biomedical applications: a short review*. *Journal of Materials Science: Materials in Medicine*, 2014. **25**(9): p. 2215-2215.
70. Zhu, J. and R.E. Marchant, *Design properties of hydrogel tissue-engineering scaffolds*. *Expert Review of Medical Devices*, 2011. **8**(5): p. 607-626.
71. Goldrick, C., et al., *3D multicellular systems in disease modelling: From organoids to organ-on-chip*. *Front Cell Dev Biol*, 2023. **11**: p. 1083175.
72. Guven, S., et al., *Multiscale assembly for tissue engineering and regenerative medicine*. *Trends in Biotechnology*, 2015. **33**(5): p. 269-279.
73. Huepe, C., et al., *Forcing function control of Faraday wave instabilities in viscous shallow fluids*. *Physical Review E*, 2006. **73**(1): p. 016310.
74. Petta, D., et al., *Sound-induced morphogenesis of multicellular systems for rapid orchestration of vascular networks*. *Biofabrication*, 2021. **13**(1): p. 015004.
75. Chen, P., et al., *Biotunable acoustic node assembly of organoids*. *Adv Healthc Mater*, 2015. **4**(13): p. 1937-43.
76. Petta, D., et al., *Sound-induced morphogenesis of multicellular systems for rapid orchestration of vascular networks*. *Biofabrication*, 2020. **13**(1).
77. Nowak-Sliwinska, P., et al., *Consensus guidelines for the use and interpretation of angiogenesis assays*. *Angiogenesis*, 2018. **21**(3): p. 425-532.
78. Heiss, M., et al., *Endothelial cell spheroids as a versatile tool to study angiogenesis in vitro*. *The FASEB Journal*, 2015. **29**(7): p. 3076-3084.
79. Ehsan, S.M., et al., *A three-dimensional in vitro model of tumor cell intravasation*. *Integrative Biology*, 2014. **6**(6): p. 603-610.
80. Bray, L.J., et al., *Multi-parametric hydrogels support 3D in vitro bioengineered microenvironment models of tumour angiogenesis*. *Biomaterials*, 2015. **53**: p. 609-620.
81. Li, Y. and E. Kumacheva, *Hydrogel microenvironments for cancer spheroid growth and drug screening*. *Science Advances*, 2018. **4**(4): p. eaas8998.
82. Brassard-Jollive, N., et al., *In vitro 3D Systems to Model Tumor Angiogenesis and Interactions With Stromal Cells*. *Front Cell Dev Biol*, 2020. **8**: p. 594903.
83. Magdeldin, T., et al., *Engineering a vascularised 3D in vitro model of cancer progression*. *Scientific Reports*, 2017. **7**(1): p. 44045.
84. Tetzlaff, F. and A. Fischer, *Human Endothelial Cell Spheroid-based Sprouting Angiogenesis Assay in Collagen*. *Bio Protoc*, 2018. **8**(17): p. e2995.
85. Rezzola, S., et al., *In vitro and ex vivo retina angiogenesis assays*. *Angiogenesis*, 2014. **17**(3): p. 429-42.
86. Staton, C.A., et al., *Current methods for assaying angiogenesis in vitro and in vivo*. *Int J Exp Pathol*, 2004. **85**(5): p. 233-48.
87. Chen, P., et al., *Microscale assembly directed by liquid-based template*. *Adv Mater*, 2014. **26**(34): p. 5936-41.
88. Medicine, S.D.E.f.R. *Product Data Sheet 24-Well Plate*. 2024 30/9/2024]; Available from: <https://www.sp5d.com/cm/wp-content/uploads/Kugelmeiers-Datasheet-SP5D24.pdf>.